The Pennsylvania State University

The Graduate School

Department of Materials Science and Engineering

REVISED MODELS OF THE CONTACT ACTIVATION BLOOD PLASMA-COAGULATION CASCADE

A Thesis in

Materials Science and Engineering

by

Harit Pitakjakpipop

Submitted in Partial Fulfillment
of the Requirements
for the Degree of

Master of Science

August 2017

The thesis of Harit Pitakjakpipop was reviewed and approved* by the following:

James H. Adair
Professor of Materials Science and Engineering, Bioengineering and Pharmacology
Thesis Advisor

Ralph H. Colby
Professor of Materials Science and Engineering and Chemical Engineering

James P. Runt
Professor of Polymer Science

Suzanne Mohney
Professor of Materials Science and Engineering and Electrical Engineering
Chair, Intercollege Graduate Degree Program in Materials Science and Engineering

*Signatures are on file in the Graduate School

ABSTRACT

About 25 percent of Americans are currently living with some form of cardiovascular disease with approximately 800,000 deaths each year. Millions of cardiovascular devices are used each year in the US. However, all biomaterials eventually lead to some form of thrombosis. Therefore, surface engineering of biomaterials with improved hemocompatibility is an imperative, given the widespread global need for cardiovascular devices. Investigating the biochemical reaction of blood factor proteins in contact with an activation surface is the major purpose of these studies. Research summarized in this thesis focuses on contact activation of *FXI* and *FXII* in buffer and blood plasma, a process usually referred to as *autoactivation*.

In Chapters 2 and 3, recent hematology literature combined with new theoretical and experimental results from our laboratory offers an updated version of blood plasma coagulation cascade biochemistry *in vitro* for use in the study of blood-biomaterial interactions. A revised version of the coagulation cascade is proposed that emphasizes a known role for *FXI* in controlling the time required to complete plasma coagulation after activation with hydrophilic procoagulant surfaces such as glass. Central to this revision is a "thrombin (*FIIa*) amplification route" that has been generally recognized in existing models of *in vivo* plasma coagulation cascade biochemistry but has been afforded the proper emphasis as a pivotal feedback loop that activates *FXI in vitro*, in a way similar to that known to occur *in vivo*. Thus, a connection between *in vitro* and *in vivo* coagulation is drawn. We propose that this thrombin amplification route is catalyzed by the substantial amount of *FIIa* generated in coagulating plasma that persists in serum prepared from coagulated plasma. This revision (Fig. 3.4) further includes an updated version (Fig. 3.5) of the contact activation phase mediated by surface activation of the Hageman factor known as *FXII*.

In Chapter 4, a contact activation of *FXII* in buffer solutions (i.e. in absence of plasma proteins) with hydrophilic and silanized-glass activators spanning the observed range of water

wettability (hydrophilic to hydrophobic), shows no evidence based on high-resolution electrophoresis evaluating proteolytic cleavage of *FXII* into *αFXIIa* or *βFXIIa*. The autoactivation mixture contains only a single-chain protein with a molecular weight of ~80 kDa, confirming the previous finding of Oscar Runoff of a single-chain activated form of *FXII* that he called 'HFea'. Functional assays have shown that these autoactivation products exhibit procoagulant potential (protease activity inducing clotting of blood) or amidolytic potential (cleaves amino bonds in s-2302 chromogen but do not cause coagulation of plasma) or both amidolytic potential and procoagulant potential. Some of these proteins also have the remarkable potential to 'suppress autoactivation' (i.e. suppress creation of enzymes with procoagulant potential). It is thus hypothesized that autoactivation of *FXII* in the absence of plasma proteins generates not just a single type of activated conformer, as suggested by previous researchers, but rather an ensemble of conformer products with collective activity that varies with activator surface energy used in contact activation of *FXII*. Furthermore, reaction of *αFXIIa* with *FXII* in buffer solution does not produce additional *αFXIIa* by the putative autoamplification reaction *FXII* + *FXIIa* → *2FXIIa* as has been proposed in past literature to account for the discrepancy between chromogenic and plasma-coagulation assays for *αFXIIa* in buffer solution. Instead, net procoagulant activity measured directly by plasma-coagulation assays decreases systematically with increasing *FXII* solution concentration. Under the same reaction conditions, chromogenic assay reveals that net amidolytic activity increases with increasing *FXII* solution concentration. Thus, although autoamplification does not occur, it appears that there is some form of "*FXII* self-reaction" that influences the products of *αFXIIa* reaction with *FXII*. Electrophoretic measurements indicate that no proteolytic cleavage takes in this reaction leading us to conclude that change in activity is most likely due to change(s) in *FXII* conformation (with related change in enzyme activity).

TABLE OF CONTENTS

LIST OF FIGURES

LIST OF TABLES

GLOSSARY AND SYMBOLS

Amidolytic activity	The protein produced by autoactivation of FXII in buffer solution
βFXIIa	Human Coagulation *Factor βXIIa* enzymes
CT	Coagulation Time
ºC	Degrees Celsius
dl	Deciliter
Fibrin ferment	A white, albuminous, fibrous substance, formed in the coagulation of the blood which makes its appearance in the blood shortly after it is shed
FXII	Human Coagulation *Factor XII* (Hageman Factor)
FXIIa	Human Coagulation *Factor XII* enzymes
αFXIIa	Human Coagulation *Factor αXII* enzymes
g	grams
kg	Kilograms
M	Molarity
m^3	Cubic meters
mg	Milligrams
min.	Minutes
mL	Milliliters
mm	Millimeters
MΩ	Mega Ohms (10^6 Ohms)
MW	Molecular Weight
n	Number
ng	Nanograms (10^{-9} g)
OTS	Octadecyltrichlorosilane
PBS	Phosphate Buffered Saline

PEU	Plasma Equivalent Units
pg	Picogram (10^{-12} g)
PK	Prekallikrein
HMWK	High-Molecular Weight Kininogen
PPP	Human platelet poor plasma
Procoagulant	An inactive coagulation protein that becomes activated during the coagulation process to form a serine protease or cofactor and produce a fibrin clot
SA	Surface area
sec.	Seconds
µg	Micrograms
µl	Microliters
µm	Micrometers

ACKNOWLEDGEMENTS

I would like to express my gratitude to my graduate advisors, Dr. Erwin Vogler and Dr. James Adair, whose guidance was indispensable for my master research. Dr. Vogler has been a mentor and friend to me, and I have learned much about science, life, and philosophy from him.

Many thanks are due to my dissertation committee members Dr. James Runt, and Dr. Ralph Colby, for taking out the time to critically review this work. Their enthusiastic and encouraging comments kept me going and were of tremendous value to the dissertation.

I am grateful to my colleagues, Dr. Avantika Golas, Dr. Naris Barnthip, and Dr. Qiaoling Huang for their valuable help and suggestions, and for fostering an enjoyable lab environment.

This dissertation is dedicated to my family, and I want to thank them for constantly pushing me towards worthwhile pursuits. My wife Pawnprapa Pitakjakpipop made my journey very special.

This work was supported by National Institute of Health grant PHS 5R01HL069965. Authors appreciate support from the Departments of Bioengineering and Materials Science and Engineering, The Pennsylvania State University.

Chapter 1

Introduction

1.1 Cardiovascular healthcare

Cardiovascular disease is one of four-main types of non-communicable diseases with approximately 800,000 deaths each year in the US. About 2,200 American die of cardiovascular disease every day and around 92.1 million adults are living with some form of cardiovascular disease or after-effects of stroke. Stroke ranks No. 4 among all cause of death in the US, killing nearly 133,100 people in 2016 [1]. Consequently, performance of cardiovascular medical devices such as vascular grafts, heart valves, and pumps commonly requires a long-term anticoagulation with attendant health problems. However, a limitation is that blood coagulates to some extent in contact with all known biomaterials.

From an economic standpoint, there are millions of units of hemocompatible devices used worldwide. The U.S. leads the world production of medical devices with a value of 140 billion dollars in 2016. Cardiovascular disease costs estimated amount of more than $300 billion (Table 1.1) in the United States alone. Thus, there is a need for biomaterials with improved hemocompatibility for advanced cardiovascular medical devices[2].

Table 1.1. Estimated Direct and Indirect Costs (in Billions of Dollars) of CVD and Stroke: United States, Average Annual 2012 to 2013 [1]

	Heart Disease	**Stroke**	**Hypertensive Disease**	**Other Circulation Condition**	**Total Cardiovascular Disease**
Direct costs‡					
Hospital inpatient stays	55.1	10.0	7.2	16.0	88.3
Hospital ED visits	5.4	1.0	1.7	1.1	9.2
Hospital outpatient or office-based provider visits	20.1	2.0	13.3	6.1	41.5
Home health care	8.3	3.9	5.4	0.7	18.3
Prescribed medicines	9.8	1.0	19.7	1.9	32.4
Total expenditures	98.7	17.9	47.3	25.8	189.7
Indirect costs§					
Lost productivity/mortality	100.9	16.0	3.9	5.6	126.4
Grand totals	199.6	33.9	51.2	31.4	316.1

Although sophisticated medical devices and technology are available, the host reactions with blood contacting materials via complex biological responses are not well understood. Cardiovascular biomaterials require structure-property relationships linking blood coagulation with material properties including surface chemistry/energy. Potentiation of the blood plasma coagulation cascade by surface contact activation of the blood zymogen *Factor XII* (*FXII*, Hageman factor) is thought to be a cause of the relatively poor hemocompatibility of all currently known cardiovascular biomaterials [3]. Two enzymes, *αFXIIa*, and *βFXIIa*, have been identified as products of *FXII* activation with protease activity inducing clotting of blood plasma (procoagulant activity). These enzymes initiate the intrinsic pathway of coagulation that ultimately causes blood or blood plasma transition from the liquid phase to gel (blood clot) phase.

1.2 Objectives and Thesis structure

The objective of the work presented in this thesis is to investigate the mechanism and revise the model of the blood coagulation cascade for contact activation of plasma *in vitro*. The studies involved assembly of proteins comprising an "activation complex" on activating surfaces mediated by specific chemical interactions among activation complex proteins and the surface. This activation complex was thought to consist of *FXII* (Hageman factor), prekallikrein (*PK*), high-molecular-weight kininogen (*HMWK*), and Factor IX(*FIX)*, Factor X(*FX)* and Factor XI (*FXI)* (see 3D structure of Blood factors in Appendix A). This thesis is divided into 5 chapters with the overarching hypothesis that *a complete contact blood coagulation cascade promotes revision around the molecular mechanism of autoactivation which new approaches for surface engineering biomaterials with improved hemocompatibility.*

Chapter 1 provides a brief cardiovascular healthcare recent situation, objectives and thesis structure, and the significance of the studies.

Chapter 2 gives a review of blood coagulation and chronicles discovery of various blood factors. A revised version of the blood coagulation cascade is presented to emphasize the revision for the proposed role of *FXI* and the thrombin amplification pathway.

Chapter 3 investigates the blood plasma coagulation times promoted by additions of *FIX*, *FX*, and *FXI* for a range of glass particle activation doses via increasing surface area of glass-particle activator. The hypothesis for Chapter 3 is *that supplemental blood factors (FIX, FX, and FXI) in plasma will clarify the role/function of FXII and thrombin (FIIa).* We found that only FXI plays a role in controlling the time required for complete plasma coagulation after activation with procoagulant surfaces such as glass. This led us to propose a "*FIIa* amplification route" that activates *FXI in vitro* is present in a manner similar to that occurring *in vivo*.

Chapter 4 identifies the protein produced in *FXII* activation via high-resolution electrophoresis analysis and chromogenic assay in buffer by the putative autoamplification reaction $FXII \xrightarrow{\substack{activator \\ surface}} FXII_{act}$ in the absence and present of prekallikrein (*PK*), and high-molecular-weight kininogen (*HMWK*). If *FXII* autoactivation in buffer is to occur, then *the amidolytic potential and procoagulant potential will be found in the reaction* $FXII \xrightarrow{\substack{activator \\ surface}} FXII_{act}$. However, high-resolution electrophoresis of autohydrolysis products did not show evidence of proteolytic cleavage of either *FXII* or *αFXIIa*. Therefore, it is likely that the surface autoactivation

is mediated by a different mechanism: the possibility of *FXII* conformational change at surfaces is one of the possible mechanisms.

Chapter 5 provides conclusions and future work.

Appendix A - 3D Crystal Structures of Blood Coagulation Factors.

Appendix B - describes how we calculated autoactivation yield in plasma from an *FXIIa* titration.

Appendix C - expands how propagated error was calculated for the data with an example calculation.

Appendix D - Schematic of Silane molecular structures.

1.3 Significance

The current theory of blood plasma coagulation is inconsistent with recent experimental findings. This work offers significant revisions to the existing theory and new finding of contact activation of *FXII* and a role of *FXI* after activation with hydrophilic procoagulant surface such as glass in buffer for an updated vision of the contact activation phase mediated by surface activation of Hageman Factor (*FXII)*. This, in turn, provides potential avenues for surface engineering of biomaterials such as heart valve and stent with enhanced hemocompatibility, thus reducing the morbidity and costs associated with the usage of cardiovascular devices.

1.4 References

1. Benjamin EJ, Blaha MJ, Chiuve SE, Cushman M, Das SR, Deo R, et al. Heart Disease and Stroke Statistics—2017 Update: A Report from the American Heart Association. Circulation. 2017.
2. Vogler EA, Siedlecki CA. Contact Activation of Blood Plasma Coagulation: A Contribution from the Hematology at Biomaterial Interfaces Research Group the Pennsylvania State University. Biomaterials. 2009;30(10):1857-69.
3. Roberts HR. Oscar Ratnoff: His Contributions to the Golden Era of Coagulation Research. British Journal of Haematology. 2003;122(2):180-92.

Chapter 2

Background

2.1 Blood and Blood Proteins

Human blood is a suspension of formed elements or cells, in plasma, an aqueous solution containing a variety of organic or inorganic constituents and more than 3,400 proteins [1]. An average adult has a blood volume of approximately 5 liters, with females normally having less blood volume than males which is regulated by the kidneys.

Plasma is a clear straw-yellow liquid composed of about 90% water, 8% plasma proteins, 1.1% organic substances and 0.9% inorganic ions [2]. Table 2.1 list the major coagulation proteins and their concentrations in the normal human. Around 3,400 plasma proteins have been accounted for, with serum albumin (3.5-5 g/dl) ranking the highest concentration following by serum globulin (1.0-1.5 g/dl), and fibrinogen (0.2-0.45 g/dl). Many proteins are only present in deficient levels (< pg/ml), owing to introduction by low-level tissue leakage [3]. All plasma proteins perform differently ranging from transportation of macromolecules to coagulation of human blood.

Table 2.1. Plasma coagulation factors[4]

Factor	Common Name	Molecular Weight (kDa)	Plasma Concentration (mg/dl)
FI	Fibrinogen	340	200-400
FII	Prothrombin	72	12
FIII	Tissue thromboplastin [a]	-	-
FIV	Divalent calcium ion[b]	-	2.2-2.5 mEq/l
FV	Proaccelerin (labile factor)	330	0.4-1.4
FVI	Not assigned	-	-
VII	Proconvertin (stable factor)	48	0.05-0.06
VIII	Antihemophilic factor	1000-12000	0.5-1
IX	Christmas factor	57	0.4-0.5
X	Stuart-Prower factor	59	0.7-1.2
XI	Plasma thromboplastin antecedent	160	0.4-0.6
XII	Hageman factor	80	1.5-4.5
XIII	Fibrin stabilizing factor	320	1-2
Plasma Prekallikrein	Fletcher factor	88	3.5-4.5
High-molecular weight kininogen	Fitzgerald, Williams, or Flaujeac factor	120	8-9
Plasminogen	-	92	20

a. A lipoprotein complex principally located on cell membranes with 50 < MW < 330 kDa

b. Total plasma calcium = 8.5-10.5 mg/dl

c. FVI is no longer considered to be a coagulant following the discovery that FVI is actually an activated form of FV

2.2 Blood coagulation

Blood coagulation proceeds through a number of zymogen-enzyme conversions; this sequence of events is known as the coagulation cascade [4], shown in Figure 2.1. The intrinsic, extrinsic, and common pathways are the three main pathways of the cascade and the control systems that mediate fibrinolysis and formation of thrombus. Coagulation is a cascade of zymogen-enzyme conversions; therefore, the enzyme or product of one reaction can activate other inactive molecules in the cascade and can quickly amplify into thrombus formation.

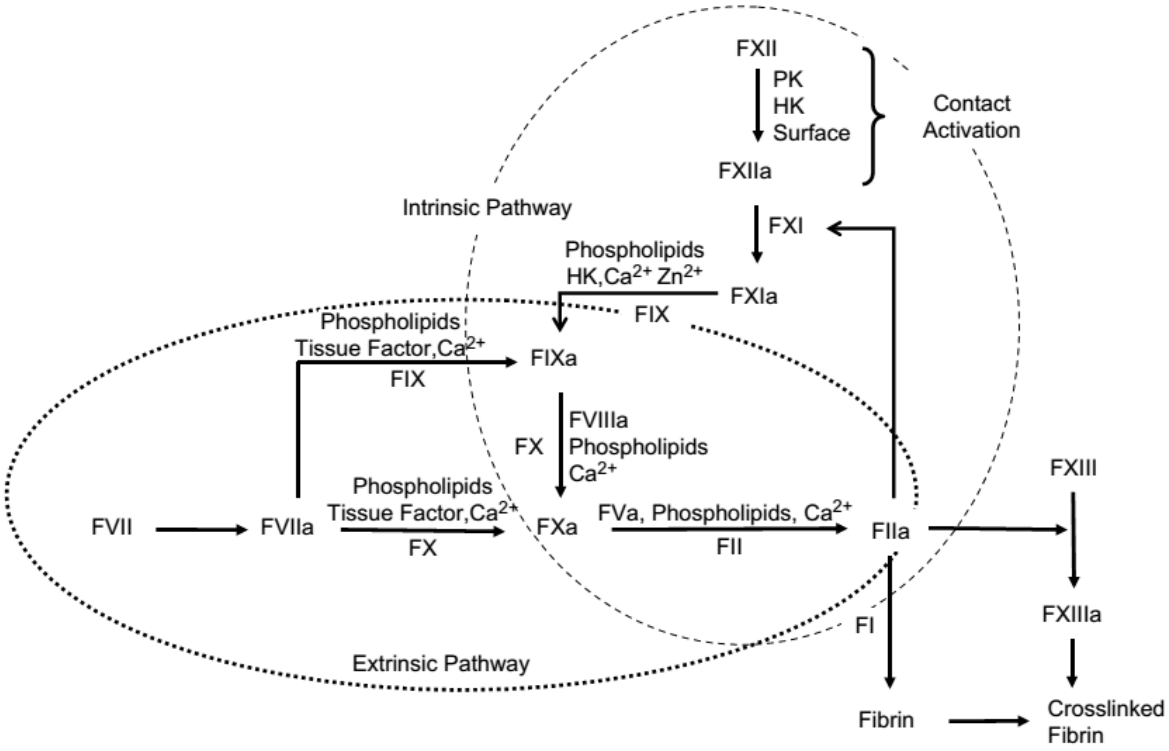

Figure 2.1 A modern and generally-accepted model of the blood coagulation cascade divided into intrinsic and extrinsic pathways that converge into a common pathway given by the intersection of the intrinsic and extrinsic pathway ellipses in which *FXI* is hydrolyzed into *FXIa* by thrombin (FIIa). See ref [4] and citations therein.

Mammals have a process to stop bleeding called hemostasis that maintains blood in the vascular system from a vessel injury. There are three main stages-platelet plug formation and vasoconstriction, activation of biochemical cascade that generates a fiber network called fibrin meshwork, and finally fibrinolysis. The first stage, after the vessel is damaged, the platelets accumulate and form a plug at the site of vascular injury. The platelet plug formation is accompanied by vasoconstriction which limits local circulation to reduce bleeding. The second stage, the series of biochemical events in blood-plasma form a fibrin meshwork, which stabilizes the platelet plug. Finally, as wound healing continues, the fibrin plug is attacked and its fragments are removed by phagocytosis [5].

Thrombosis is the pathological formation of a blood clot inside a blood vessel, preventing the flow of blood through the circulatory system. Even when a blood vessel is not injured, the blood clot may form and can break off from the site (embolus) and get lodged at distant sites causing vascular occlusion and subsequent pathologies. Thrombosis may occur if the intensity of the hemostatic stimulus exceeds the capacity of the inhibitory system, or if the inhibitory system is impaired in some way.

2.2.1 Genesis of the waterfall/cascade model of blood coagulation

The earliest references to blood coagulation date back to Greek scientists at about 400 BC. Hippocrates, the father of western medicine, observed that the blood of a wounded soldier congealed and the bleeding stopped when ‘coagulum skin’ covered the wound. Aristotle noted that blood cooled and congealed when removed from the body (see the time line of important events summarized in Figure. 2.2). Thus the ‘cooling’ hypothesis of blood coagulation was postulated (i.e. blood coagulates when cooled). In 1770, William Hewsen described the clotting process and demonstrated that the coagulum comes from the liquid portion of blood [6]. Later, in the 1790s,

John Hunter postulated that clotting occurs on exposure of blood to air and not cooling as proposed earlier [7]. In 1832, Johannes Muller first described fibrin, and Rudolph Virchow named its soluble precursor, fibrinogen. Prosper Sylvain Denis isolated fibrinogen in 1856 and subsequently Alexander Schmidt inferred the presence of a substance that converted fibrinogen to fibrin [8]. Schmidt concluded that this fibrin ferment (which he called thrombin) is formed from an inactive zymogen (later identified as prothrombin) by cellular factors and subsequently converts fibrinogen into fibrin [9, 10]. In 1890, Arthus and Pages observed that calcium precipitants inhibit coagulation, thus establishing the essential role of calcium (later called Factor IV). Based on this evidence, in 1904, Morawitz postulated that free calcium ions were required for coagulation [11]. Platelets were identified in 1865 by Max Schultze, and their function was elucidated by Giulio Bizzozero, who observed them microscopically in 1882 [12, 13]. In 1905, Paul Morawitz assembled coagulation factors into a schema by demonstrating that in the presence of calcium, tissue thromboplastin (later called Factor III), and prothrombin (later called Factor II) was converted into thrombin which subsequently converted fibrinogen (later called Factor I) into a fibrin clot. Patek and Taylor discovered *Factor VIII* in 1939. In that same year, Brinkhaus showed that patients with hemophilia were deficient in a plasma factor he called anti-hemophillic factor.

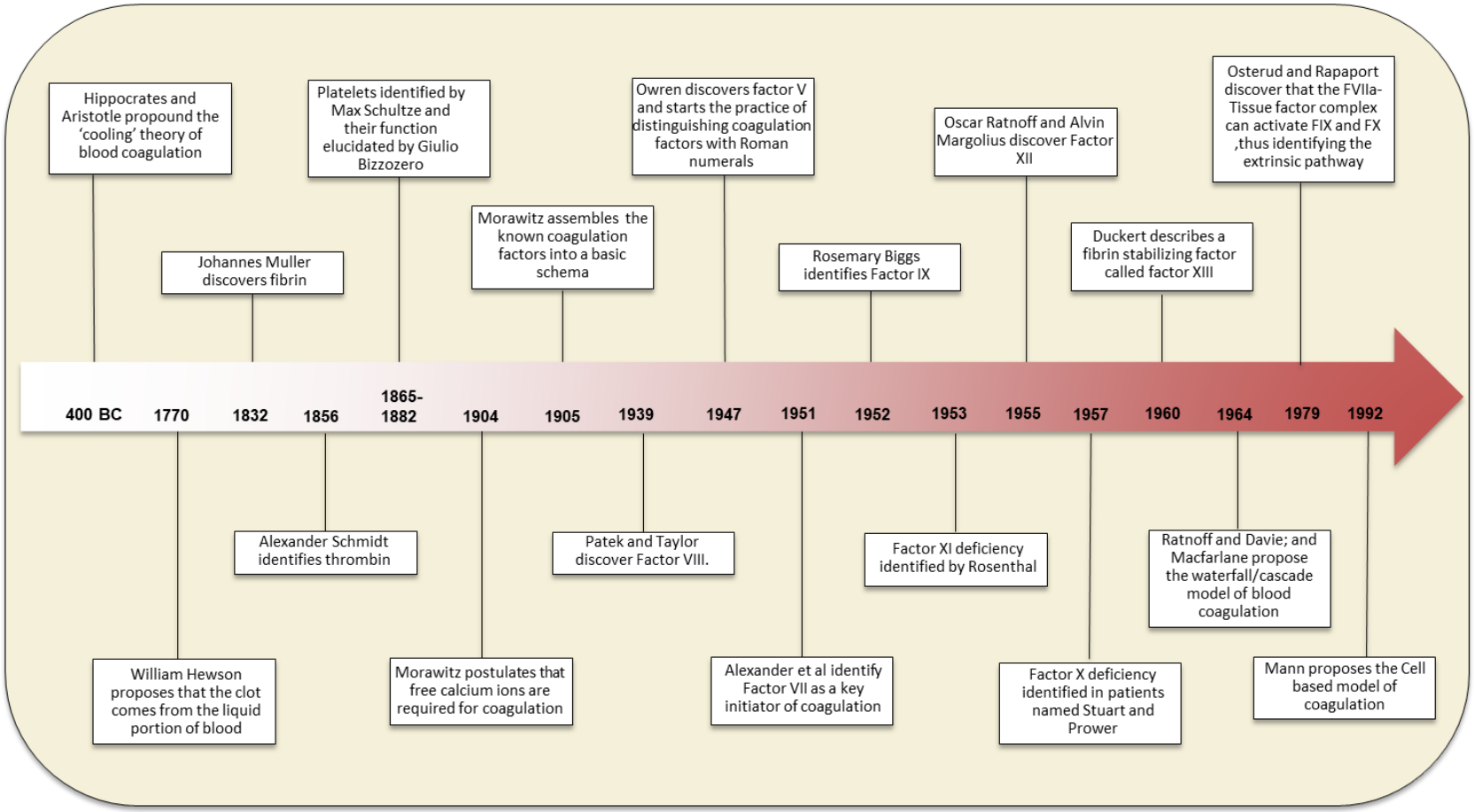

Figure 2.2 Milestones in the understanding of blood-plasma coagulation (to be read in conjunction with discussion in Section 2.2.1 [6-15].

In 1952, Loeliger named this protein Factor VIII. Owren, following his discovery of Factor V in 1947 [5], started the practice of distinguishing coagulation factors with Roman numerals. In 1951, Alexander *et al* identified Factor VII as the key initiator of coagulation and reported the first case of Factor VII *(FVII)* deficiency in a child, calling it serum prothrombin conversion accelerator deficiency [14]. Factor IX (*IX*) was discovered in 1952, by Rosemary Biggs, and was called Christmas factor after the patient Stephen Christmas. Factor XI deficiency was described in 1953 by Rosenthal, and by 1954, the coagulation model was on its way to acquiring its familiar cascade/waterfall form [4, 5] (Figure 2.1). *FXII* was discovered by Oscar Ratnoff and Alvin Margolius in 1955, when they observed, but did not ignore, a curious phenomenon in the blood of three patients; a gentleman named John Hageman, and two sisters unrelated to Hageman [15].

In each case, the blood from these patients exhibited a prolonged coagulation time, about three times longer than ordinarily observed in both glass and siliconized tubes. These observations were made more-or-less by chance as these patients exhibited no bleeding diathesis or hemorrhagic episodes that would otherwise have suggested a coagulopathy responsible for slow coagulation. Bearing with these clinical observations, these investigators eventually isolated a protein missing in these patients' blood, which they named Hageman factor [15, 16] after John Hageman. Factor X deficiency was identified in 1957 in patients named Stuart and Prower. In 1960, Ducker *et. al*. described fibrin stabilizing factor (Factor XIII), thus completing the identification all the known factors that participate in the coagulation cascade. Since these factors were not uniformly named, an international committee was established in 1954 to harmonize the nomenclature. Roman numerals were assigned at various meetings held between 1955 to 1963 [17]. Factors III and VI remained unassigned because thromboplastin was not yet identified and accelerin was found to be activated Factor V.

In 1964, Ratnoff and Davie proposed the waterfall hypothesis for blood coagulation. MacFarlane contemporaneously proposed a similar scheme, which he referred to as the 'cascade'

model of blood coagulation [18-20]. Both cascade and waterfall models are patterned as a series of linked zymogen/enzyme conversions that eventually terminate in the hydrolysis of fibrinogen to fibrin, which then crosslinks into a coagulum (clot). The waterfall model did not explicitly mention separately identifiable extrinsic and intrinsic pathways, and the cascade model only briefly touched upon the subject. In 1979, Osterud and Rapaport discovered that *FVIIa*-Tissue factor complex (*TF-FVIIa*) could activate *FIX* and *FX*, thus leading to the identification of an extrinsic pathway [21]. In the 1990s, Gailani and Broze demonstrated that clotting *in vivo* is initiated by *TF-FVIIa* and that contact activation factors of the intrinsic pathway were not essential for physiological hemostasis [22]. The cascade was eventually divided into the extrinsic and intrinsic pathways that converge into a common pathway with the activation of Factor X to Factor Xa.

The intrinsic pathway initiates via the contact-activation system whereas the extrinsic pathway is initiated by tissue factor (*TF*), a membrane protein present in subendothelial cells. Following vascular injury, blood-plasma comes in contact with the exposed tissue factor (TF) present in the blood-vessel wall. Tissue factor forms a complex with Factor VIIa, resulting in a *TF-FVIIa* complex that activates Factor IX, which in turn activates Factor X, completing convergence with the common pathway (Figure 2.1).

The intrinsic pathway initiates by way of a contact-activation complex that includes high-molecular-weight kininogen (*HMWK*), Prekallikrein (*PK*), Factor XI(*FXI*), and importantly Factor XII *(XII)*. More recently, a cell-based model taking into account participation of blood platelets *in vivo* has brought about an important incremental advance in the evolution of our understanding of the coagulation process (see further section 2.2.4) that helps reconcile *in vivo* and *in vitro* coagulation. Yet another step forward has been the study of real-time *in vivo* homeostasis that reveal intricate details of the blood coagulation process that do not necessarily occur *in vitro* [22].

2.2.2 Contact-activation of blood-plasma coagulation

Contact-activation is the first step in the intrinsic pathway of blood coagulation, and refers to the conversion of *FXII* to *FXIIa* following 'contact' with an activating surface. Involvement of prekallikrein(*PK*) in contact activation was shown by Wuepper and Cochrane in 1972 [23]. This was followed by systematic studies by Cochrane, Revak, Bagdasar, and Colman *et al.* established that kallikrein acted as a proteolytic activator of *FXII*, [23-26]. Cochrane and Griffin proposed a mechanistic scheme for contact activation in the late 1970's, which has become the commonly accepted or 'consensus mechanism' of contact activation. According to this scheme, *Factor XII* binds to a negatively charged surface, which renders it susceptible to cleavage. Involvement of *HMWK* in the contact-activation reaction was established subsequently [27-31]. The *HMWK-PK* complex purportedly binds to the activating surface as well, cleaving *FXII* into either *αFXIIa* (which is thought to remain bound to the activating surface) or *βFXIIa* (presumably released in solution). In turn, *FXIIa* activates *PK* to kallikrein, purportedly remaining bound to the surface as an *HMWK-FXI* complex which ultimately releases *FXIa*. Accordingly, all molecules are brought into reactive proximity that multiply yield of *FXIIa* through 'reciprocal amplification.' *FXIa* converts *Factor IX* to *IXa*, which then merges into the common pathway (see Figure.2.1).

Traditional hematology literature proposes the idea that contact-activation is most efficiently activated by "anionic hydrophilic" surfaces such as kaolin, clay, glass or generally any material with an oxidized surface chemistry [4]. Systematic studies aimed at quantifying the relationship between surface chemistry, surface energy, and contact activation by Vogler *et al.* [32-34] showed that whereas activation was most efficient (as measured by the time to coagulate plasma) for hydrophilic activators (a.k.a. procoagulants exhibiting water contact angle ~0°), coagulation efficiency was sharply reduced for less water-wettable surfaces (hydrophobic procoagulants, water contact angle >65°) [32, 34]. Thus, a sharp hydrophilic/hydrophobic contrast

in blood coagulation was quantified. Contact activation of blood-plasma coagulation was thus said to be specific to hydrophilic anionic activator surfaces, where specificity refers to Cochrane and Griffin's proposition that an activation complex of proteins assembles on anionic surfaces through surface-chemical (presumably Lewis acid-base type interactions). This specificity of *FXII* for anionic surfaces was hypothesized to be due to chemical binding between positive charges (lysine clusters) on the surface of *FXII*, and negative charges on the anionic procoagulant surfaces [4, 35]. It has also been suggested that *HK* possesses anionic binding domains, which bring *HK* and *FXI* into an orientation favorable to activation [4, 36].

However, work done in our lab over the last decade or so has shown that contact-activation *in vitro* differs significantly from the aforementioned hypotheses. Zhuo *et al* [37] demonstrated that autoactivation in neat-buffer solutions was nearly equal with both hydrophobic and hydrophilic procoagulants, as measured by solution yield of enzymes with procoagulant properties (a.k.a. apparent *FXIIa* activity). Zhuo thus concluded that contact-activation with hydrophobic surfaces in plasma appears relatively sluggish due to "competitive" adsorption of a multitude other blood proteins found in significantly higher concentrations than *FXII* in plasma, which block *FXII* adsorption to, or collisions with, the physical activator surface. Parhi *et al* [38] significantly extended these findings to surfaces incrementally sampling the full range of observable water-wettability and found similar results. Moreover, it was discovered that autoactivation of *FXII* in neat-buffer solution produces at least three distinct categories of activated proteins, with each category possibly subsuming a family of fragments/conformers. The relative proportions of these categories were found to depend on activator surface chemistry/energy [39].

Chatterjee *et al* [40] observed that, contrary to the traditional hypothesis, prekallikrein hydrolysis is not localized to an activation complex on the procoagulant surface. Furthermore, *FXII* is found not to formally adsorb to hydrophilic surfaces (*i.e.* concentrate within the interphase of hydrophilic surfaces), only transiently encountering the hydrophilic interphase region [4, 41].

Here, interphase refers to that region surrounding an activator surface that separates the physical procoagulant surface from solution. Instead, it is proposed that *FXII* molecules pass through this interphase region by random diffusion/thermal motion [42] without formally adsorbing to the procoagulant surface. Close encounter of *FXII* with the surface is apparently sufficient to activate *FXII* [29, 32]. but water strongly bound to hydrophilic surfaces cannot be displaced by proteins to become adsorbed [42]. These findings, all taken together, raise serious questions about the viability of the molecular assembly model proposed by Cochrane and Griffin [57].

2.2.3 Cell-Based Model of Blood Coagulation

In 1992, Mann proposed what is now called the "cell-based model" of coagulation [22]. The model has an initiation phase, which begins when *TF* forms a complex with circulating *FVIIa* resulting in the generation of a relatively small amount of *FIIa*, and a propagation phase, where the most of the *FIIa* is generated. Some researchers also propose an amplification phase.

FVII circulates in both inactive and active form (*FVIIa*), with the active form constituting approximately 1% of the total *FVII* in human plasma [22]. *FVII* can undergo activation by *FIXa*, *FXa*, *FXIIa*, (*FIX*, *FX*, or *FXII* proteolytic enzymes) *FIIa*, plasmin, or *FVIIa* activating protease, but its most potent physiological activator is currently unknown [22]. Once the *TF-FVIIa* complex is formed, it activates *FIX* to *FIXa*, and subsequently, *FX* to *FXa*, resulting in the generation of a trace amount of *FIIa* (the 'initiation' phase). A *TF-FVIIa-FXa* complex is rapidly neutralized by inhibitors and further *FIIa* generation is dependent on the success of the propagation phase. The inhibitors, TFPI (tissue factor pathway inhibitor) and *anti-FIIa* (ATIII) thus "police" the process in case of a false alarm. Trace amounts of *FIIa* diffuse away and cleave *FXI* to *FXIa*. *FV* is converted to *FVa* on the surface of platelets recruited to the site of vascular damage (the 'amplification' phase). Von Willebrand factor (vWF) is cleaved from *FVIII* by *FIIa* and *FVIII* then activates to

FVIIIa. In the 'propagation' phase, *FIXa*, along with *FVIIIa*, binds to a platelet membrane, forming the tenase complex (*FIXa*, *FVIIIa*, *FX*, and calcium). The tenase complex activates *FX* to *FXa*, which accounts for the majority of *FXa* formed physiologically. *FXa* precipitates assembly of the *pro-FIIaase* complex (*FVa*, *FXa*, and calcium). The *pro-FIIaase* complex results in a burst of *FIIa* and subsequent formation of a fibrin clot.

2.2.4 Factor XII and its role in blood-plasma coagulation

Hageman factor as it was called in the 1950's, or *Human Blood Factor XII*, EC = 3.4.21.38 [43] is central to the plasma surface contact-activation system and widely thought to be primarily responsible for poor biomaterial hemocompatibility. *FXII* is a 596-amino acid, single-chain β globulin glycoprotein (16.8% carbohydrate), with a molecular mass of between 76-80 kDa, an isoelectric point of 6.1 to 6.5, and concentrations in human plasma ranging from 15-47 μg/ml [4, 44, 45].

The amino-acid chain sequences of *FXII* and its two primary proteolytic products, *αFXIIa* and *βFXIIa*, have been established [46] and confirmed later by examining the organization of the human *FXII* gene. 3-D crystal structures of *FXII* are not as clear, however, with only few studies conducted using computer models [47].

Evolutionarily speaking, *FXII* is a relatively new protein and is present in a number of mammalian species, but not in non-mammalian vertebrates or lower taxonomic ranks [48, 49]. *FXII* triggers the so-called intrinsic cascade as part of the plasma contact system [43, 50] that includes *Factor XII*, high molecular weight kininogen (*HMWK*), prekallikrein (*PK*) and *FXI*. Activated *FXII* triggers the classic complement pathway as well as, and the fibrinolytic system *in vitro* [51-53]. It remains uncertain, however, if *αFXIIa* has the capacity to trigger activation of the complement and fibrinolytic systems *in vivo* [43, 54]. Whereas the initial steps in contact

activation of *FXII* in the absence of plasma proteases remains uncertain [31, 45, 55], *in vitro* activation of *FXII* has been variously attributed to proteolytic cleavage [39, 56-64], change in conformation [43, 56, 65-70], or a combination of these mechanisms [45, 71].

The classic cascade model (Figure 2.2) serves as a useful reference for laboratory coagulation assays and *in vitro* studies. *FXII* is important in the study of blood-biomaterial interactions as it mediates thrombus formation on biomaterials [4, 72-74], as mentioned above. The cell-based model of coagulation suggests that *FXII* is dispensable for homeostasis and that *FXIIa/TF*-driven coagulation plays the dominant role *in vivo*. However, several new studies have dispelled the myth that *FXII* plays no role in coagulation *in vivo* [75]. Recent research shows that *FXII*-deficient mice exhibit defective pathological thrombus formation [43]. Moreover, activated *FXII* can cleave *FVII* to *FVIIa*, which is identical to that produced by *FXa* in the extrinsic pathway. Whereas *FXa* eventually digests and inactivates *FVIIa* produced, activated *FXII* leads to the formation of a stable form of *FVIIa* which can then accelerate the extrinsic pathway as it occurs in case of physiological clotting [76]. *FXII* is also suspected to be a participant in DIC (Disseminated Intravascular Coagulation) [43, 77]. Several *in vivo* contact activators of *FXII* such as polyphosphate (polyp) [78], over sulfated chondroitin sulfate, nucleotides, miss-folded protein aggregates and mast-cell heparin, have been discovered, which may be involved in thrombotic and inflammatory diseases. *FXII*, therefore, plays an important role in plasma coagulation even though its role in overall homeostasis is limited. Thus, *FXII* presents a target for anticoagulant drug design in therapeutic applications for venous thromboembolism or arterial thrombosis (myocardial infarction or stroke). *FXII*-material-surface interactions also offer therapeutic potential, such as in activator (kaolin-based) wound dressings [79].

2.3 Summary

Experiments recently conducted in our lab have discovered the following key pieces of information about *FXII* autoactivation *in* vitro [29, 32]:

1) *FXII* autoactivation in the absence of plasma proteins creates a burst of enzymes that exhibit procoagulant (protease activity inducing clotting of blood) and/or amidolytic potential (cleaves amino bonds in s-2302 chromogen but do not cause coagulation of plasma); the relative proportions of which depend on activator surface chemistry/energy.
2) This burst of enzyme(s) created upon *FXII* activation (autoactivation) in buffer is self-limiting and exhibits no measurable kinetics, sensitivity to mixing, activator-surface area dependence, or solution-temperature dependence.
3) High-resolution electrophoresis of *FXII* autoactivation proteins in neat-buffer solution does not exhibit bands indicative of proteolytic fragment formation.

All taken together, these findings indicate that autoactivation in the absence of other plasma proteins creates an ensemble of single-chain *FXII* conformers (Figure A-1). These conformers could be an intermediate step in contact-activation reactions or a protein product that plays an as-yet unknown role.

2.4 References

1. Keshishian H, Burgess MW, Gillette MA, Mertins P, Clauser KR, Mani DR, et al. Multiplexed, Quantitative Workflow for Sensitive Biomarker Discovery in Plasma Yields Novel Candidates for Early Myocardial Injury. Molecular & Cellular Proteomics. 2015;14(9):2375-93.
2. Krebs HA. Chemical Composition of Blood Plasma and Serum. Annual Review of Biochemistry. 1950;19(1):409-30.
3. Anderson NL, Polanski M, Pieper R, Gatlin T, Tirumalai RS, Conrads TP, et al. The Human Plasma Proteome: A Nonredundant List Developed by Combination of Four Separate Sources. Molecular & Cellular Proteomics. 2004;3(4):311-26.
4. Vogler EA, Siedlecki CA. Contact Activation of Blood-Plasma Coagulation. Biomaterials. 2009;30(10):1857-69.
5. Malone P.C. APS. The Coagulation Cascade and the Consensus Model of DVT. The Aetiology of Deep Venous Thrombosis: Springer; 2008. p. 11-29.
6. DAMESHEK W. Editorial—William Hewson, Thymicologist; Father of Hematology? Blood. 1963;21(4):513-6.
7. Mitchell PD, Boston C, Chamberlain AT, Chaplin S, Chauhan V, Evans J, et al. The Study of Anatomy in England from 1700 to the Early 20th Century. Journal of Anatomy. 2011;219(2):91-9.
8. Shapiro SS. Treating Thrombosis in the 21st Century. New England Journal of Medicine. 2003;349(18):1762-4.
9. Recent Advances in Thrombosis and Hemostasis. Tanaka K. DEW, editor. Japan: Springer; 2008.
10. Viles-Gonzalez JF, Fuster V, Badimon JJ. Thrombin/Inflammation Paradigms: A Closer Look at Arterial and Venous Thrombosis. American Heart Journal. 2005;149(1):S19-S31.
11. Bergsagel DE. The Role of Calcium in the Activation of the Christmas Factor. British Journal of Haematology. 1955;1(2):199-212.
12. Brewer DB. Max Schultze (1865), G. Bizzozero (1882) and the Discovery of the Platelet. British Journal of Haematology. 2006;133(3):251-8.
13. Jie Jack Li EJC. Drug Discovery: Practices, Processes, and Perspectives: Wiley; 2013.
14. Alexander B, Goldstein R, Landwehr G, Cook CD, Addelson E, Wilson C. Congenital Spca Deficiency - a Hitherto Unrecognized Coagulation Defect with Hemorrhage Rectified by Serum and Serum Fractions. Journal of Clinical Investigation. 1951;30(6):596-608.
15. Ratnoff OD, Margolius A, Jr. Hageman Trait: An Asymptomatic Disorder of Blood Coagulation. Transactions of the Association of American Physicians. 1955;68:149-54.
16. Ratnoff OD, Rosenblum JM. Role of Hageman Factor in the Initiation of Clotting by Glass. The American Journal of Medicine. 1958;25(2):160-8.
17. Giangrande PLF. Six Characters in Search of an Author: The History of the Nomenclature of Coagulation Factors. British Journal of Haematology. 2003;121(5):703-12.
18. Davie EW, Ratnoff OD. Waterfall Sequence for Intrinsic Blood Clotting. Science. 1964;145(363):1310-&.
19. Roberts HR. Oscar Ratnoff: His Contributions to the Golden Era of Coagulation Research. British Journal of Haematology. 2003;122(2):180-92.
20. Macfarlane RG. An Enzyme Cascade in the Blood Clotting Mechanism, and Its Function as a Biochemical Amplifier. Nature. 1964;202(4931):498-9.
21. Seligsohn U, Østerud B, Brown SF, Griffin JH, Rapaport SI. Activation of Human Factor Vii in Plasma and in Purified Systems: Roles of Activated Factor Ix, Kallikrein, and Activated Factor XII. The Journal of Clinical Investigation. 1979;64(4):1056-65.

22. McMichael M. New Models of Hemostasis. Topics in Companion Animal Medicine. 2012;27(2):40-5.
23. Wuepper KD, Cochrane CG. Effect of Plasma Kallikrein on Coagulation *in-vitro*. Proceedings of the Society for Experimental Biology and Medicine. 1972;141(1):271-&.
24. Bagdasar.A, Talamo RC, Colman RW. Isolation of High Molecular-Weight Activators of Human Plasma Prekallikrein. Journal of Biological Chemistry. 1973;248(10):3456-63.
25. Bagdasar.A, Lahiri B, Colman RW. Origin of High Molecular-Weight Activator of Prekallikrein. Journal of Biological Chemistry. 1973;248(22):7742-7.
26. Wuepper KD, Cochrane CG. Plasma Prekallikrein - Isolation, Characterization, and Mechanism of Activation. Journal of Experimental Medicine. 1972;135(1):1-&.
27. Schiffma.S, Lee P. Preparation, Characterization, and Activation of a Highly Purified Factor-XI - Evidence That a Hitherto Unrecognized Plasma Activity Participates in Interaction of Factors XI and XII. British Journal of Haematology. 1974;27(1):101-14.
28. Schiffman S, Lee P. Partial-Purification and Characterization of Contact Activation Cofactor. Journal of Clinical Investigation. 1975;56(5):1082-92.
29. Schiffman S, Lee P, Waldmann R. Identity of Contact Activation Cofactor and Fitzgerald Factor. Thrombosis Research. 1975;6(5):451-4.
30. Chan JYC, Habal FM, Burrowes CE, Movat HZ. Interaction between Factor-XII (Hageman-Factor), High Molecular-Weight Kininogen and Prekallikrein. Thrombosis Research. 1976;9(5):423-33.
31. Espana F, Ratnoff OD. Activation of Hageman-Factor (Factor-XII) by Sulfatides and Other Agents in the Absence of Plasma Proteases. Journal of Laboratory and Clinical Medicine. 1983;102(1):31-45.
32. Vogler EA, Graper JC, Harper GR, Sugg HW, Lander LM, Brittain WJ. Contact Activation of the Plasma Coagulation Cascade I. Procoagulant Surface Chemistry and Energy. Journal of Biomedical Materials Research. 1995;29:1005-16.
33. Vogler EA, Graper JC, Sugg HW, Lander LM, Brittain WJ. Contact Activation of the Plasma Coagulation Cascade.2. Protein Adsorption on Procoagulant Surfaces. J Biomed Mat Res. 1995;29:1017-28.
34. Vogler EA, Nadeau JG, Graper JC. Contact Activation of the Plasma Coagulation Cascade. Iii. Biophysical Aspects of Thrombin-Binding Anticoagulants. Journal of Biomedical Materials Research. 1998;40(1):92-103.
35. Josh Yeh CH, Dimachkie ZO, Golas A, Cheng A, Parhi P, Vogler EA. Contact Activation of Blood Plasma and Factor Xii by Ion-Exchange Resins. Biomaterials. 2012;33(1):9-19.
36. Golas A, Yeh C-HJ, Pitakjakpipop H, Siedlecki CA, Vogler EA. A Comparison of Blood Factor XII Autoactivation in Buffer, Protein Cocktail, Serum, and Plasma Solutions. Biomaterials. 2013;34(3):607-20.
37. Zhuo R, Siedlecki CA, Vogler EA. Autoactivation of Blood Factor XII at Hydrophilic and Hydrophobic Surfaces. Biomaterials. 2006;27(24):4325-32.
38. Parhi P, Golas A, Barnthip N, Noh H, Vogler EA. Volumetric Interpretation of Protein Adsorption: Capacity Scaling with Adsorbate Molecular Weight and Adsorbent Surface Energy. Biomaterials. 2009;30(36):6814-24.
39. Golas A, Yeh CHJ, Siedlecki CA, Vogler EA. Amidolytic, Procoagulant, and Activation-Suppressing Proteins Produced by Contact Activation of Blood Factor XII in Buffer Solution. Biomaterials.32(36):9747-57.
40. Chatterjee K, Thornton JL, Bauer JW, Vogler EA, Siedlecki CA. Moderation of Prekallkrein-Factor XII Interactions in Surface Activation of Coagulation by Protein-Adsorption Competition. Biomaterials. 2009;30(28):4915-20.

41. Vogler EA. Surface Modification for Biocompatibility. Lakhtakia A, Martin-Palma, R. J., editor. New York: Elsevier; 2011.
42. Vogler EA. Protein Adsorption in Three Dimensions. Biomaterials. 2012;33(5):1201-37.
43. Maas C, Oschatz C, Renne T. The Plasma Contact System 2.0. Seminars in Thrombosis and Hemostasis.37(4):375-81.
44. Colman RW, Schmaier AH. Contact System: A Vascular Biology Modulator with Anticoagulant, Profibrinolytic, Antiadhesive, and Proinflammatory Attributes. Blood. 1997;90(10):3819-43.
45. Pixley RA, Colman RW. Factor-XII - Hageman-Factor. Proteolytic Enzymes in Coagulation, Fibrinolysis, and Complement Activation, Part A. 1993;222:51-65.
46. Fujikawa K, Walsh KA, Davie EW. Isolation and Characterization of Bovine Factor-XII (Hageman-Factor). Biochemistry. 1977;16(10):2270-8.
47. Henriques ES, Floriano WB, Reuter N, Melo A, Brown D, Gomes J, et al. The Search for a New Model Structure of Beta-Factor XIIa. Journal of Computer-Aided Molecular Design. 2001;15(4):309-22.
48. Ratnoff OD. The Evolution of Hemostatic Mechanisms. Perspectives in Biology and Medicine. 1987;31(1):4-33.
49. Ponczek MB, Gailani D, Doolittle RF. Evolution of the Contact Phase of Vertebrate Blood Coagulation. Journal of Thrombosis and Haemostasis. 2008;6(11):1876-83.
50. Jackson CM, Nemerson Y. Blood-Coagulation. Annual Review of Biochemistry. 1980;49:765-811.
51. Ratnoff OD. Activation of Factor-Xi. Blood. 1993;81(12):3483-4.
52. Nemerson Y, Furie B. Zymogens and Cofactors of Blood-Coagulation. Crc Critical Reviews in Biochemistry. 1980;9(1):45-85.
53. Ratnoff OD. Why Does the Blood Not Coagulate. Western Journal of Medicine. 1993;158(2):195-6.
54. Ratnoff OD. Surface-Mediated Defenses against Injury. Archives of Dermatology. 1983;119(5):432-7.
55. Bock PE, Srinivasan KR, Shore JD. Activation of Intrinsic Blood-Coagulation by Ellagic Acid - Insoluble Ellagic Acid-Metal Ion Complexes Are the Activating Species. Biochemistry. 1981;20(25):7258-66.
56. Revak SD, Cochrane CG, Johnston AR, Hugli TE. Structural-Changes Accompanying Enzymatic Activation of Human Hageman-Factor. Journal of Clinical Investigation. 1974;54(3):619-27.
57. Revak SD, Cochrane CG, Bouma BN, Griffin JH. Surface and Fluid Phase Activities of 2 Forms of Activated Hageman-Factor Produced During Contact Activation of Plasma. Journal of Experimental Medicine. 1978;147(3):719-29.
58. Dunn J, Silverberg M, Kaplan A. The Cleavage and Formation of Activated Human Hageman-Factor by Autodigestion and by Kallikrein. Journal of Biological Chemistry. 1982;257(4):1779-84.
59. Dunn J, Kaplan A. Formation and Structure of Human Hageman-Factor Fragments. The Journal of clinical investigation. 1982;70(3):627-31.
60. Dunn JT, Silverberg M, Kaplan AP. Structural-Changes Accompanying Hageman-Factor Activation by Proteolysis. Clinical Research. 1982;30(2):A315-A.
61. Miller G, Silverberg M, Kaplan AP. Autoactivatability of Human Hageman-Factor (Factor-XII). Biochemical and Biophysical Research Communications. 1980;92(3):803-10.
62. Dunn JT, Silverberg M, Kaplan AP. The Cleavage and Formation of Activated Human Hageman Factor by Autodigestion and by Kallikrein. J Biol Chem. 1982;257(4):1779-84.

63. Silverberg M, Dunn JT, Garen L, Kaplan AP. Autoactivation of Human Hageman Factor. Demonstration Utilizing a Synthetic Substrate. J Biol Chem. 1980;255(15):7281-6.
64. Vanderkamp K, Vanoeveren W. Factor-XII Fragment and Kallikrein Generation in Plasma During Incubation with Biomaterials. Journal of Biomedical Materials Research. 1994;28(3):349-52.
65. Samuel M, Pixley RA, Villanueva MA, Colman RW, Villanueva GB. Human Factor-XII (Hageman-Factor) Autoactivation by Dextran Sulfate - Circular-Dichroism, Fluorescence, and Ultraviolet Difference Spectroscopic Studies. Journal of Biological Chemistry. 1992;267(27):19691-7.
66. McMillin CR, Walton AG. Circular-Dichroism Technique for Study of Adsorbed Protein Structure. Journal of Colloid and Interface Science. 1974;48(2):345-9.
67. Griep M, Fujikawa K, Nelsestuen G. Possible Basis for the Apparent Surface Selectivity of the Contact Activation of Human-Blood Coagulation Factor-Xii. Biochemistry. 1986;25(21):6688-94.
68. McMillin CR, Saito H, Ratnoff OD, Walton AG. Secondary Structure of Human Hageman-Factor (Factor-XII) and Its Alteration by Activating Agents. Journal of Clinical Investigation. 1974;54(6):1312-22.
69. Samuel M, Samuel E, Villanueva GB. The Low Ph Stability of Human Coagulation-Factor-XII (Hageman-Factor) Is Due to Reversible Conformational Transitions. Thrombosis Research. 1994;75(3):259-68.
70. Ratnoff OD, Saito H. Amidolytic Properties of Single-Chain Activated Hageman-Factor. Proceedings of the National Academy of Sciences of the United States of America. 1979;76(3):1461-3.
71. Silverberg M, Dunn JT, Garen L, Kaplan AP. Auto-Activation of Human Hageman-Factor - Demonstration Utilizing a Synthetic Substrate. Journal of Biological Chemistry. 1980;255(15):7281-6.
72. Ratner BD. The Blood Compatibility Catastrophe. Journal of Biomedical Materials Research. 1993;27(3):283-7.
73. Ratner BD. Blood Compatibility - a Perspective. Journal of Biomaterials Science-Polymer Edition. 2000;11(11):1107-19.
74. Ratner BD. The Catastrophe Revisited: Blood Compatibility in the 21st Century. Biomaterials. 2007;28(34):5144-7.
75. Herold R, Straub PW. In-Vivo Role of Factor-XII (Hageman-Factor) in Hypercoagulability and Fibrinolysis. Journal of Laboratory and Clinical Medicine. 1972;79(3):397-&.
76. Puy C, Tucker EI, Wong ZC, Gailani D, Smith SA, Choi SH, et al. Factor Xii Promotes Blood Coagulation Independent of Factor XI in the Presence of Long-Chain Polyphosphates. Journal of Thrombosis and Haemostasis. 2013;11(7):1341-52.
77. Colman RW. Are Hemostasis and Thrombosis Two Sides of the Same Coin? Journal of Experimental Medicine. 2006;203(3):493-5.
78. Smith SA, Morrissey JH. Polyphosphate: A New Player in the Field of Hemostasis. Current opinion in hematology. 2014;21(5):388-94.
79. Kheirabadi BS, Mace JE, Terrazas IB, Fedyk CG, Valdez KK, MacPhee MJ, et al. Clot-Inducing Minerals Versus Plasma Protein Dressing for Topical Treatment of External Bleeding in the Presence of Coagulopathy. Journal of Trauma-Injury Infection and Critical Care.69(5):1062-72.

Chapter 3

Revised models of the Blood Plasma-Coagulation Cascade

3.1 Introduction

A significant challenge in the field of biomaterials is to develop a comprehensive understanding of blood-biomaterial compatibility (hemocompatibility) that identifies structure-property relationships [1] for biomaterials used in a wide variety of cardiovascular medical devices. Millions of these cardiovascular medical devices are used every year [1, 2] that save or improve countless lives, a testament to the importance of cardiovascular biomaterials. Yet, there remains no clear consensus as to which materials are truly hemocompatible or why materials are or are not hemocompatible. Importantly, it is unclear the extent to which the *in vitro* condition models *in vivo* and *vice versa.* Such an understanding requires a comprehensive model of the biochemical mechanism of the coagulation process as it occurs both *in vivo* and *in vitro.* A revised and updated mechanism is thus an imperative in formulating a strategy for the goals as mentioned above.

3.2 Methods and Materials

3.2.1 Preparation and characterization of particulate activators

Test activator surfaces used in this work were 425-600 μm diameter glass particles (Sigma Aldrich) in either cleaned or silanized form. The nominal specific area used in this work was $5x10^{-3}$ m^2/g (based on 512.5 μm mean diameter and 168 μg/particle). The surface area measured

by the Brunauer-Emmett-Teller (BET) method (Micromeritics ASAP 2000 using liquid nitrogen as the probe gas) was (8.5 ±0.1) x 10^{-3} m^2/g. Nominal surface area was used throughout this work as a matter of consistency with prior work and in recognition of the fact that surface area did not influence conclusions based on comparisons among experiments described herein using the same source of particulate activator with a fixed single specific surface area.

Glass particles and cover slips were first cleaned and activated by 30 min. immersion in heated piranha solution (30% H_2O_2 in concentrated H_2SO_4 at approximately 80 ^oC) followed by 3x sequential washes in each of 18 MΩ de-ionized water and 100% ethanol. Piranha-solution oxidized glass was air dried and subsequently oxidized by air-plasma treatment (10 min at 100 W plasma; Herrick, Whippany, NY) of a single layer of particles (or cover slip) held in a 15 mm Pyrex glass Petri dish, directly before use in blood-plasma coagulation activation measurements. Glass surfaces treated in this manner were found to be fully water wettable and designated “clean glass”.

PBS contact angles on glass cover slip witness samples were measured using an automated contact-angle goniometer (First Ten Angstroms Inc., Portsmouth, VA) that employed the captive-drop method of measuring advancing/receding contact angles (see references[3, 4] for a comparison of goniometric techniques and discussion of experimental errors). Contact angles could not be read directly on glass particles, but optical microscopy of the shape of the liquid meniscus of particles partly immersed in water on a microscope slide qualitatively confirmed that the treated particles were not different from the cover slip witness samples. Surface chemistry of glass-particle surfaces has been previously assayed using a Diffuse Reflectance Infrared Fourier Transform Spectroscopy (DRIFT) collected on a Bruker IFS-66/S Tech as described in ref. [4].

3.2.2 Plasma and coagulation proteins

Citrated human platelet poor plasma (PPP) [5] as prepared from unexpired pooled lots of blood were obtained from the M.S. Hershey Medical Center Blood Bank and prepared as described previously[1, 2, 6]. This work was performed with a single batch of PPP aliquoted into 15 ml polypropylene tubes (Falcon, Becton Dickinson) and frozen at -20 ^{o}C until use. Experiments for this work were conducted within a month of PPP preparation. Repeat trials yielded no significant variations in coagulation times within this experimental time frame.

Human *FIX*, *FX*, *FXI*, *FXII*, and *αFXIIa* were used as received from Enzyme Research Laboratories (South Bend, IN). Activity of *FIX*, *FX*, *FXI*, *FXII*, and *αFXIIa* were specified by the vendor in mg/mL or traditional units of plasma equivalent units per mL (PEU/mL). A neat-buffer solution of *αFXIIa* solution was prepared in phosphate buffer saline (PBS; Sigma; 0.14M NaCl, 3mM KCL prepared from powder in 18MΩ de-ionized water, Plasma-supplemented with *FXI* was prepared by adding 38.8 µL of *FXI* (at the vendor-provided concentration of 3.60 mg/mL) to 2.5 mL plasma. Similarly, plasma supplemented with *FXI* and *FIX* was prepared by adding 38.8 µL of *FXI* (at the vendor-provided concentration of 3.60 mg/mL) and 8.07 µL of FIX (at the vendor-provided concentration of 5.25 mg/mL) to 2.5 mL plasma. Plasma-supplemented with *FXI*, *FIX* and *FX* were prepared by adding 38.8 µL of *FXI* (at the vendor-provided concentration of 3.60 mg/mL), 8.07 µL of *FIX* (at the vendor-provided concentration of 5.25 mg/mL) and 3.86 µL of *FX* (at the vendor-provided concentration of 8.20 mg/mL) to 2.5 mL plasma.

We test this simple kinetics idea by monitoring the apparent yield of *FXIIa* obtained by activating normal human plasmas supplemented with *FIX*, *FX*,*FXI*, (F9, F10 ,11) as a function of 'procoagulant dose' (increasing surface area of SiOx glass particles, known to activate plasma coagulation [1]). As is evident from Figure 3.1 and 3.2 and previous similar studies [1, 4, 7, 8] *FXIIa* yield increases as coagulation time (CT) falls, apparently following two kinetic phases,

leading to a lower-level CT asymptote as *FXIIa* exponentially rises to an upper level asymptote, each in the continuous presence of activator surface area.

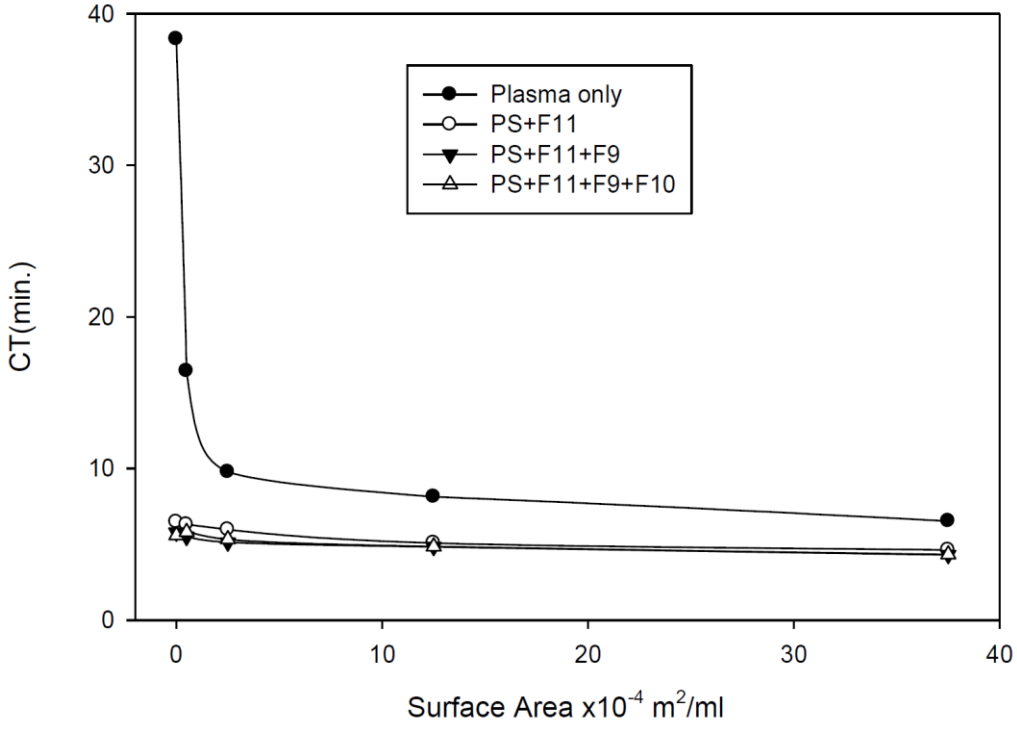

Figure 3.1 Hydrophilic glass-particle activator surface area titration (SAT) of normal human plasma (PS, filled circles) plotting coagulation time CT (ordinate) against activator surface area (abscissa) compared to factor-supplemented plasmas: (exogenous *FXI*, open circles), *FIX* and *FXI* (F9 and 11, filled inverted triangles) and *FXI*, *FX*, and *FIX* (F11, 10, F9, unfilled triangles). Notice that CT is significantly shorter when plasma is supplemented with F11 but that addition of *FIX* or *FX* seems to have little discernible affect over-and-above *FXI* alone. Decreasing CT with increasing contact activation (increasing procoagulant surface area, abscissa) parallels increasing endogenous FXIIa production (see Figure 3.2). We propose shortening of CT in *FXI* supplemented plasma is due to the 'thrombin amplification' route.

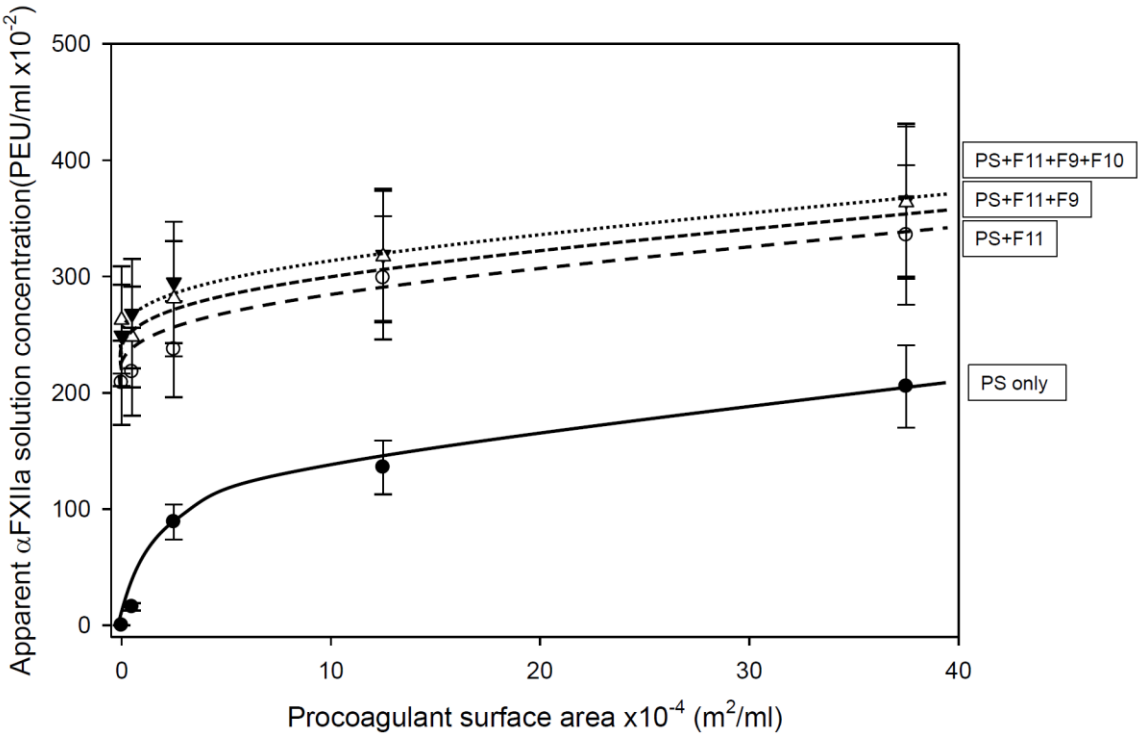

Figure 3.2 Apparent *FXIIa* concentration increases with increasing glass particle activation dose (increasing surface area of glass-particle activator) for normal human plasma (PS, filled circles) and factor supplemented plasmas: exogenous *FXI*, open circles; *FIX* and *FXI* (F9 and 11, filled inverted triangles); and *FXI*, *FX*, and *FIX* (F11, 10, F9, unfilled triangles). CT values were converted to apparent *FXIIa* concentrations using the calibration curve of Figure 3.3. Notice that CT is significantly shorter when plasma is supplemented with F11(presumably due to the accelerating effect of the thrombin amplification route shown in section 2.3) but that addition of *FIX* or *FX* seems to have little discernible affect over-and-above *FXI* alone, compare to Figure 3.1 lines through the data are guides to the eye.

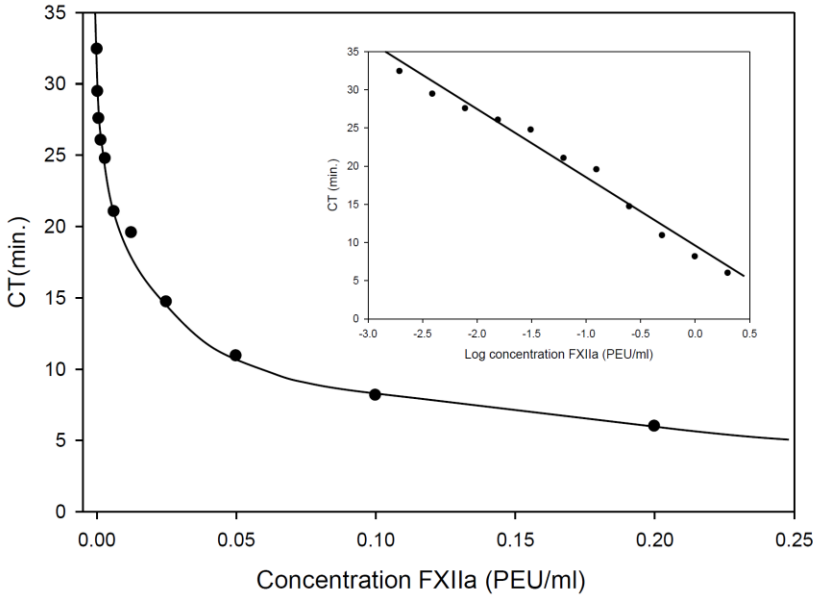

Figure 3.3 *FXIIa* titration of human plasma, plotting observed plasma coagulation time (CT, ordinate) against exogenous *FXIIa* concentration (abscissa). The asymptotic curve is linear on logarithmic axes (inset), creating a convenient calibration curve that allows estimation of apparent *FXIIa* concentration from measured CT. Lines through the data are guides to the eye.

3.2.3 *in vitro* coagulation assay

An *in vitro* coagulation assay was used to measure plasma coagulation time (CT) after activation with particulate activator. CT was the time required for liquid plasma to undergo a phase transition from liquid to gel rheology in a tube slowly rotating on a hematology mixer (10 rounds per minute, Roto-shake Genie, Scientific Industries Inc.). CT measurements were obtained by mixing 0.5 ml of platelet poor plasma (PPP), optionally supplemented with exogenous blood factors, 0.1 ml of 0.1 M calcium chloride ($CaCl_2$, Sigma-Aldrich), and procoagulant surface (ranging from 0.0 to 4.0 x 10^{-4} m^2) to assay vials. A final volume of 1 ml was reached by addition of 0.01 M phosphate buffered saline (PBS, pH = 7.4 at 25 $^{\circ}$C, Sigma-Aldrich). Assay vials were capped with parafilm, rotated at 8 rpm on a hematology mixer, and the CT was recorded.

3.3 Role of FIIa in the Cell-based Model

Among the many publications constituting a burgeoning literature on the subject of blood coagulation, we find [9] to perhaps be the most meaningful toward revising a scheme for the coagulation cascade. This work shows that thrombin (*FIIa*) enters the cascade at a higher position than in the standard scheme. The standard scheme (Figure. 3.4) shows *FIIa* solely produced from pro-FIIa (*FII*) by the action of *FXa* on *FII* whereas new evidence suggests that FIIa is formed in "traveling waves" and can hydrolyze *FXI* to *FXIa* (Figure 3.5), intersecting the cascade roughly in the middle of the waterfall. One reason that this is important, beyond revision of the standard cascade, is that many anticoagulants target *FIIa* (DNA and protein aptamers, for example [10, 11] and citations therein), for which it is important to fully appreciate the identity and concentrations of other proteins that can bind *FIIa* in competition with a *FIIa*-binding anticoagulant.

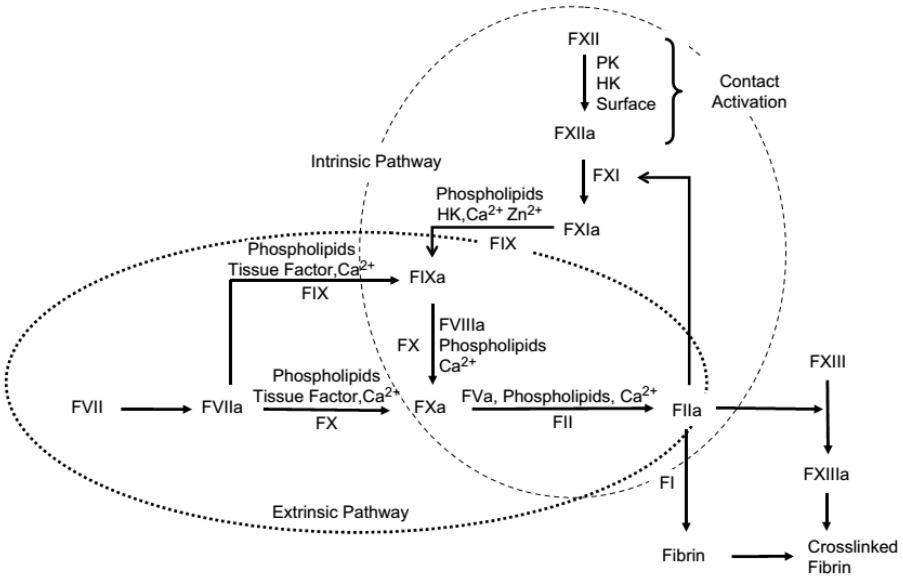

Figure 3.4 A modern and generally-accepted model of the blood coagulation cascade divided into intrinsic and extrinsic pathways that converge into a common pathway [1].

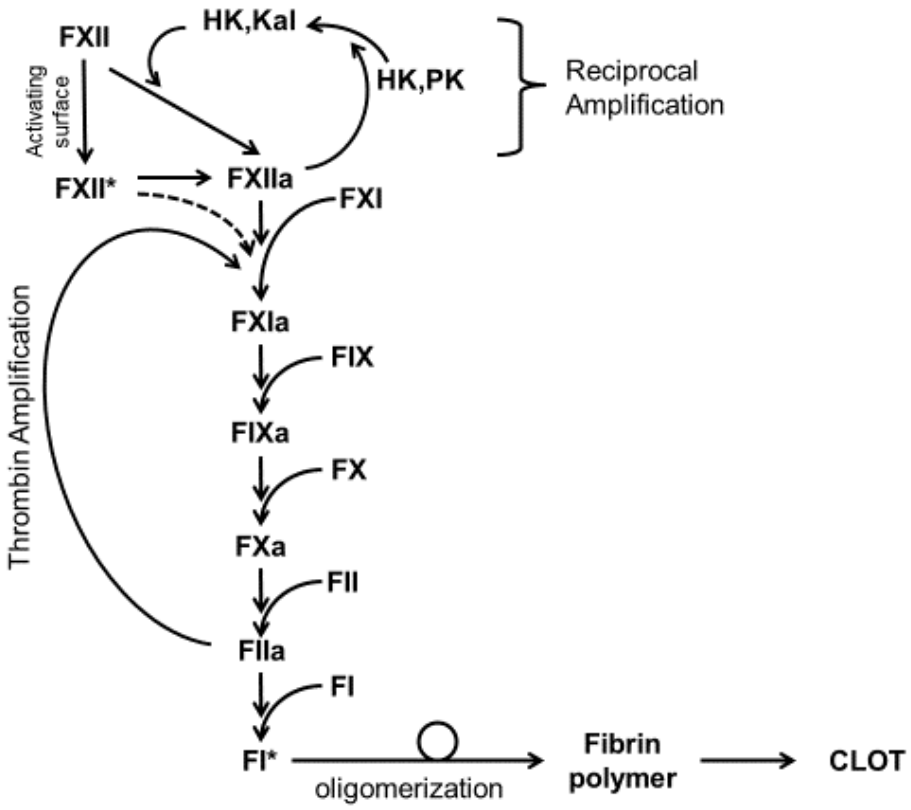

Figure 3.5 A revised version of Figure 3.4 excluding *FVII* and associated extrinsic pathway biochemistry emphasizing a "thrombin amplification pathway" (left side of figure) in which thrombin hydrolyzes *FXI* to *FXIa* as proposed to occur *in vivo*, suggesting an *in vitro* role for thrombin similar to that occurring in *in vivo* hemostasis. Exclusion of *FVII* and the extrinsic pathway focuses attention on the intrinsic pathway of Figure. 3.4 deemed important for *in vitro* blood/biomaterial testing (see ref [1] and citations therein) and emphasizes the sequential nature of linked zymogen-enzyme conversions following surface contact activation of *FXII*. This contact activation scheme is commonly viewed as essential to eliminate for improved hemocompatibility of blood-contacting biomaterials and has been updated pursuant to new experimental evidence to include production of *FXII**, an activated *FXII* conformer that can undergo subsequent hydrolysis in the presence of HK and/or PK to produce procoagulant enzymes of the *FXIIa* lineage (to be read in conjunction with the discussion in Section 2.2.2). Direct hydrolysis of *FXI* by *FXII** is proposed in this model but has not yet been demonstrated experimentally and thus remains speculative. Overall, this model incorporates *FXI* into the intrinsic cascade in a more profound manner than suggested by the simple branch point in the lower-right of Fig. 3.4 (to be read in conjunction with the discussion in Section 3.5).

Moreover, it has been shown that *FIIa* can produce additional *FIIa* [12], which presumably protects an embolus from excessive fibrinolysis and can sustain *FIIa* generation[12]. The resulting rapid spatial "procoagulant signal" propagation [13] can cross-significant distances in a heterogeneous media such as plasma, by analogy to neural impulse propagation [12]. It is important to note from the above perspective that *FIIa* waves can be a potentially dangerous dynamic factor in thrombotic diseases such atherosclerosis, trauma, stroke, infarction, cancer, and sepsis. Up to 70% of sudden cardiac deaths are due to thrombosis, killing ~800,000 people annually in the United States alone [14]. *FIIa*-dependent *FXI* activation feedback is core to sustaining *FIIa* waves and thus might be a target of antithrombotic drugs.

Figure. 3.6, scheme A presents a modified model of *FXII* autoactivation that emphasizes change in conformation as a key event. Upon contact with a material surface *in vitro*, *FXII* undergoes a change in conformation to a form herein identified as *FXII**. *FXII** has limited procoagulant potential that is sufficient to result in clot formation *in vitro*. *FXII**, in turn, exhibits enhanced susceptibility to cleavage by kallikrein, resulting in the formation of *αFXIIa* which then participates in reciprocal activation. Alternatively, as presented in Figure 3.6 scheme B, *FXII** is formed as in schematic A, but in this case, kallikrein directly cleaves much of the native molecule into its activated suite before it undergoes change in conformation. Therefore, *FXII** is not here viewed as an intermediary, but one of the primary constituents of the autoactivation suite. Actual events in plasma may well be a mix of these two schematics.

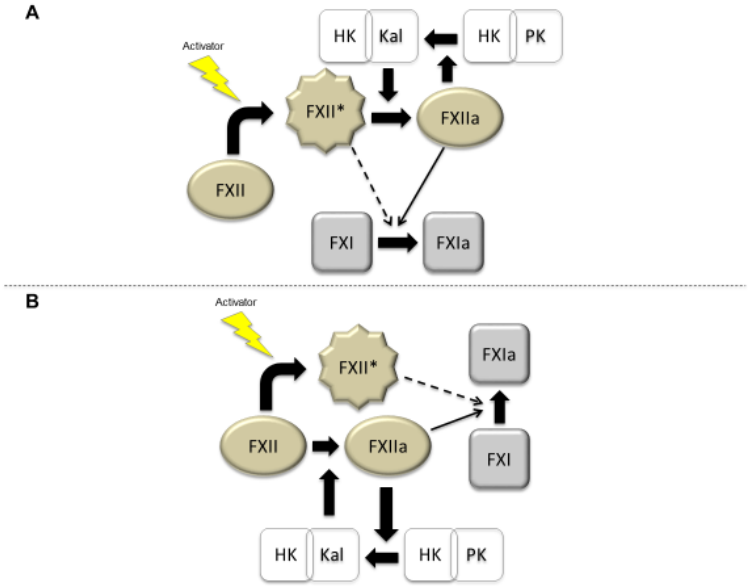

Figure 3.6 Updated contact *FXII* surface-contact activation (autoactivation) scheme that emphasizes change in *FXII* conformation as a key event. Upon contact with a material surface *in vitro*, *FXII* undergoes a change in conformation to a form herein identified as *FXII**. *FXII** has limited procoagulant potential that is sufficient to result in clot formation *in vitro*. *FXII**, in turn, exhibits enhanced susceptibility to cleavage by kallikrein, resulting in the formation of αFXIIa which then participates in reciprocal activation. Alternatively, as presented scheme B, *FXII** is formed as in schematic A, but in this case, kallikrein directly cleaves much of the native molecule into the *FXIIa* activated suite before it undergoes change in conformation. Therefore, *FXII** is not here viewed as an intermediary, but one of the primary constituents of the autoactivation complex. Actual events in plasma may well be a mix of these two schematics.

3.4 The Central Role of FXI in Plasma Coagulation

It is apparent from the cell-based model (subsection 2.2.3) that *FXI* plays a pivotal role in *in vivo* coagulation when activated by a burst of thrombin generated by platelets. We propose that this "thrombin amplification" (Figure 3.5) occurs *in vitro* as well, due to the large amount of *FIIa* generated in coagulating plasma [1]. Even when viewed from the perspective of the simplified version of the plasma cascade (Figure 3.4), it can be anticipated that *FXI* plays a more pivotal role in cascade propagation than widely thought. Figure 3.5 abstracts Figure 3.4 into a succession of zymogen activations (abscissa) arbitrarily measured as concentration ratios to nominal *FXII*

concentration (ordinate). Inspection of Figure 3.5 reveals that *FXI* is conspicuous among the other zymogens comprising of the intrinsic pathway of plasma coagulation in that *FXI* is a decade more dilute in plasma than the preceding zymogen in the activation sequence (*FXII*). All other subsequent zymogens in the activation sequence increase in concentration by at least two-fold, culminating with *FI* that is five-fold more concentrated than *FII*, which in turn, is a decade more concentrated than *FX*. This zymogen concentration profile has significant ramifications in controlling how 'procoagulant signal' arising at *FXII* autoactivation propagates down the intrinsic pathway, ultimately leading to plasma coagulation.

The familiar Michaelis-Menten (MM) formulation for the velocity V of an enzyme-catalyzed reaction $V = k_2[E]_{tot}\left(\frac{[S]}{K_M+[S]}\right) = V_{max}\left(\frac{[S]}{K_M+[S]}\right)$ has two well-known and noteworthy boundary conditions that depend on the magnitude of substrate concentration [S] relative to the MM constant K_M. If $[S]>>K_M$, then $V \rightarrow V_{max} = k_2[E]_{tot}$ where k_2 is a rate constant characteristic of the particular enzyme and $[E]_{tot}$ the total enzyme concentration. By contrast, if $[S]<< K_M$, then $V \rightarrow \left(\frac{V_{max}[S]}{K_M}\right) = C[S]$, where C is a constant particular to the enzyme. These boundary conditions suggest that *FXIIa* hydrolysis of *FXI* undergoes two kinetic phases dependent on autoactivation yield.

At low autoactivation yield in plasma, say <1%, it is evident from Figure 3.2 that [FXIIa]<<[FXI] and *FXI* hydrolysis is more like the former substrate-saturated boundary condition than the latter substrate-limited condition with $V_{max} = \left(\frac{d[FXIa]}{dt}\right) \rightarrow k_{12a}[FXIIa]$, where k_{12a} is the rate constant particular to *FXIIa*. In this regime, rate of *FXIa* production$\left(\frac{d[FXIa]}{dt}\right)$ increases in proportion to autoactivation yield. As autoactivation yield rises to >10%, however, it is evident from Figure 3.2 that [FXIIa] →[FXI] and FXI hydrolysis enters a kinetic regime more like the above substrate-limited case for which $V = \left(\frac{d[FXIa]}{dt}\right) \rightarrow C[FXI]$. This regime becomes

increasingly enforced as [FXI] decreases with progressive hydrolysis by *FXIa*. Of course, details of this proposed kinetic-regime transition depend critically on the exact balance of zymogen/enzyme concentrations in plasma and actual magnitude of MM kinetic constants, but it seems inevitable that the nominal plasma-zymogen concentrations must lead to substrate-limited kinetics in *FXI* hydrolysis (grey band in Figure 3.7), even at modest *FXII* autoactivation yield.

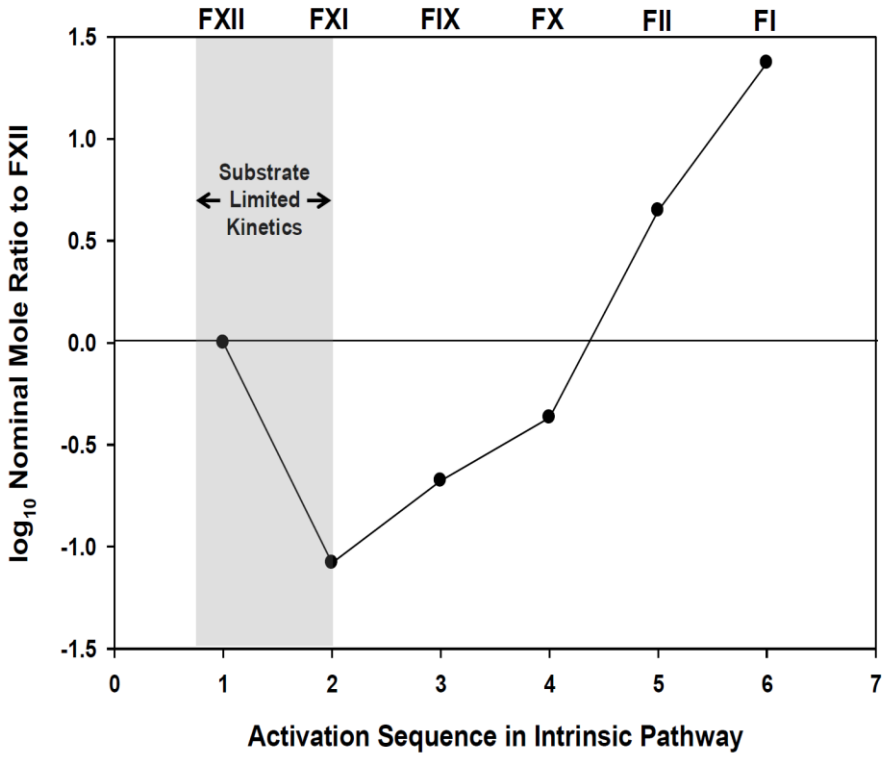

Figure 3.7 Abstraction of Figure 3.1 and 3.2 into a succession of zymogen activations (abscissa) arbitrarily measured as concentration ratio to blood Factor XII physiological concentration (ordinate) showing that *FXI* is conspicuous among other zymogens of the cascade in that *FXI* is a decade more dilute in plasma than the preceding zymogen in the activation sequence (FXII), creating a kinetic 'bottle neck' to procoagulant signal propagation down the intrinsic cascade. This coagulation-rate- limiting bottle neck can be substantially resolved by the "thrombin amplification" pathway of Figure 3.5 especially when plasma is supplemented with exogenous *FXI* as shown in Figure. 3.1 and 3.2.

3.5 Discussion

In the standard waterfall/cascade model (Figure 3.4), *FXI* can be activated by *FXIIa*, suggesting that *FXIIa* deficiency should lead to a tendency toward bleeding. Curiously though, severe *FXIIa* deficiency is not associated with bleeding in humans, cats, or mice [15] . However, in humans, *FXI* deficiency is associated with severe bleeding in surgery and trauma, suggesting an additional mechanism of *FXI* activation *in vivo* [15]. Naito [16] and Gailani [17] were apparently the first investigators to demonstrate *FXI* activation by FIIa.

On the basis of these findings, it was proposed that *FXI* activation by *FIIa* serves as a feedback mechanism to amplify the common pathway of coagulation. We emphasize this feedback loop in Figure 3.5 which connects to the reciprocal amplification loop involved in contact activation of *FXII* in the intrinsic. In this rendering, the intrinsic pathway is clearly separated from the extrinsic pathway by a common pathway comprised of the essential biochemistry that gives rise to coagulated plasma and emphasizes the central role of *FXI*, as well as the sequential activation of zymogens into proteolytic enzyme forms as in Figure 3.4. Although *FIIa* can activate *FXI*, (Figure 3.5) the process is slow and inefficient (except in the presence of PolyP) [18, 19].

Several studies have demonstrated that plasma activators of *FXI* include *FXIIa*, meizoFIIa (an intermediate of proFIIa activation) and *FXIa*. *FXIIa* and *FIIa* thus appear to be the main activators of *FXI*. It is well established that the intrinsic pathway is initiated by surface contact *in vitro* as suggested in Figure. 3.5 [1] and the final step of contact activation is *FXIIa* hydrolysis of *FXI* into *FXIa*.

Returning to Figure 3.5, it is apparent that *FXIa* and all subsequent zymogen hydrolysis reactions (*FXIa* hydrolysis of *FIX*, followed by *FIXa* hydrolysis of *FX*, followed by *FXa* hydrolysis of *FII*, followed by *FIIa* hydrolysis of *FI*) would be saturated with substrate because the zymogens are all more concentrated than the enzyme produced in the preceding activation step, even if

enzymes are produced at high yield. Under these circumstances, it is reasonable to suppose that enzyme reactions subsequent to *FXIIa* hydrolysis of *FXI* proceed under a kinetic regime more like $V \rightarrow V_{max} = k_2[E]_{tot}$, passing the '*FXIIa* procoagulant stimulus' through the intrinsic pathway at the highest possible rate. Under these circumstances, *FXIa* hydrolysis would be overall rate-limiting step in the intrinsic pathway, ultimately controlling the rate of fibrin production as well as observed plasma coagulation time CT; a bottle neck.

3.6 Conclusions:

Thorough investigation of the recent literature including new experimental results from our laboratories leads to the conclusion that the standard or consensus model of the blood-plasma coagulation cascade (Figure 3.4) needs revision. We herein offer one such revision (Figure 3.5) that highlights the role of *FXI* in controlling time required to complete plasma coagulation after activation with procoagulant surfaces such as glass. We propose a "*FIIa* amplification route" that activates *FXI in vitro*, in a way similar to that occurring *in vivo* hemostasis, drawing a connection between *in vitro* and *in vivo* coagulation. It is proposed that this amplification route is mediated by the substantial amount of *FIIa* generated in coagulating plasma that persists in serum.

3.7 References

1. Vogler EA, Siedlecki CA. Contact Activation of Blood-Plasma Coagulation. Biomaterials. 2009;30(10):1857-69.
2. Ratner BD. The Catastrophe Revisited: Blood Compatibility in the 21st Century. Biomaterials. 2007;28(34):5144-7.
3. Krishnan A, Liu YH, Cha P, Woodward R, Allara D, Vogler EA. An Evaluation of Methods for Contact Angle Measurement. Colloids and surfaces B, Biointerfaces. 2005;43(2):95-8.
4. Golas A, Parhi P, Dimachkie ZO, Siedlecki CA, Vogler EA. Surface-Energy Dependent Contact Activation of Blood Factor XII. Biomaterials. 2010;31(6):1068-79.
5. Cattaneo M, Lecchi A, Zighetti ML, Lussana F. Platelet Aggregation Studies: Autologous Platelet-Poor Plasma Inhibits Platelet Aggregation When Added to Platelet-Rich Plasma to Normalize Platelet Count2007 2007-05-01 00:00:00. 694-7 p.
6. Recent Advances in Thrombosis and Hemostasis. Tanaka K. DEW, editor. Japan: Springer; 2008.
7. Golas A, Pitakjakpipop H, Rahn MS, Siedlecki CA, Vogler EA. Enzymes Produced by Autoactivation of Blood Factor XII in Buffer: A Contribution from the Hematology at Biomaterial Interfaces Research Group. Biomaterials. 2015;37:1-12.
8. Golas A, Yeh C-HJ, Pitakjakpipop H, Siedlecki CA, Vogler EA. A Comparison of Blood Factor Xii Autoactivation in Buffer, Protein Cocktail, Serum, and Plasma Solutions. Biomaterials. 2013;34(3):607-20.
9. Hoffman M, Monroe III DM. A Cell-Based Model of Hemostasis. Thrombosis and Haemostasis. 2001;85(6):958-65.
10. Nadeau JG, Vogler EA, inventors; Becton Dickinson and Company, assignee. Rapidly Reversed Thrombin Binding Oligonucleotide Anticoagulants. USA patent 5,882,870. 1999 March, 16.
11. Nadeau JG, Vogler EA, Ciolkowski ML, Mitchell MJ, Hsieh HV. Bi-directional Oligonucleotides that bind Thrombin. Nucleic Acid Res. 1997;submitted 1997.
12. Dashkevich NM, Ovanesov MV, Balandina AN, Karamzin SS, Shestakov PI, Soshitova NP, et al. Thrombin Activity Propagates in Space During Blood Coagulation as an Excitation Wave. Biophysical journal. 2012;103(10):2233-40.
13. Zhuo R, Miller R, Bussard KM, Siedlecki CA, Vogler EA. Procoagulant Stimulus Processing by the Intrinsic Pathway of Blood Plasma Coagulation. Biomaterials. 2005;26:2965-73.
14. Go AS, Mozaffarian D, Roger VL, Benjamin EJ, Berry JD, Borden WB, et al. Heart Disease and Stroke Statistics—2013 Update: A Report from the American Heart Association. Circulation. 2013;127(1):e6-e245.
15. He R, Chen D, He S. Factor XI: Hemostasis, Thrombosis, and Antithrombosis. Thrombosis Research. 2012;129(5):541-50.
16. Naito K, Fujikawa K. Activation of Human Blood Coagulation Factor XI Independent of Factor XII. Factor XI Is Activated by Thrombin and Factor Xia in the Presence of Negatively Charged Surfaces. Journal of Biological Chemistry. 1991;266(12):7353-8.
17. Gailani D, Broze GJ, Jr. Factor XI Activation in a Revised Model of Blood Coagulation. Science. 1991;253(5022):909-12.
18. Puy C, Tucker EI, Wong ZC, Gailani D, Smith SA, Choi SH, et al. Factor XII Promotes Blood Coagulation Independent of Factor Xi in the Presence of Long-Chain Polyphosphates. Journal of Thrombosis and Haemostasis. 2013;11(7):1341-52.

19. Smith SA, Morrissey JH. Polyphosphate: A New Player in the Field of Hemostasis. Current opinion in hematology. 2014;21(5):388-94.

Chapter 4

Enzymes produced by autoactivation of blood factor XII in buffer

4.1.0. Introduction

Potentiation of the blood-plasma coagulation cascade by surface contact activation of the blood zymogen Factor XII (*FXII*, Hageman factor) is thought to be a cause of the relatively poor hemocompatibility of all currently known cardiovascular biomaterials. Two enzymes, *αFXIIa*, and *βFXIIa*, have been identified as products of *FXII* activation with protease activity inducing clotting of blood plasma (procoagulant activity). These enzymes initiate the intrinsic pathway of coagulation that ultimately causes blood or blood plasma to undergo a phase transition from liquid to gel (i.e. coagulate or clot, see Ref. [1] and citations therein that generally support this section). In spite of extensive research effort over the last five decades, *FXII* surface activation (a.k.a. autoactivation) remains a mysterious reaction with the unusual characteristics listed below recently revealed by functional assays measuring enzyme activity of the mixture produced by *FXII* autoactivation with particulate activators spanning a full range of surface chemistry/energy [2-5].

*Chapter published as dual primary authors[1]

Golas A[1], **Pitakjakpipop H[1]**, Rahn MS, Siedlecki CA, Vogler EA. Enzymes Produced by Autoactivation of Blood Factor XII in Buffer: A Contribution from the Hematology at Biomaterial Interfaces Research Group. Biomaterials. 2015; 37:1-12.

1. *FXII* autoactivation in buffer and protein solutions produces a highly variable burst of procoagulant enzyme(s) with no measurable kinetics, sensitivity to mixing, or solution-temperature dependence. Autoactivation thus appears to be a stochastic, mechanochemical-like reaction that does not exhibit the characteristics of an ordinary (bio)chemical reaction.
2. Although autoactivation is definitively initiated by surface contact, no measurable dependence on activator surface area can be discerned in buffer or protein solutions. That is to say, serial addition of activator surface area does not measurably increase procoagulant-enzyme yield.
3. Autoactivation appears to be a self-limiting reaction with an apparent procoagulant-enzyme yield converting less than 10% of starting *FXII* (at 30 μg/mL physiologic concentration) in the continuous presence of activator surface area. Thus, it appears that surface activation is somehow "shut off" after an initial catalytic event.
4. The above observations are to be contrasted to the fact that activation of blood-plasma coagulation in vitro by contact with particulate activator is demonstrably dependent on plasma-volume-to-activator-surface-area ratio.
5. *FXII* autoactivation in buffer produces an ensemble of as-yet unidentified proteins represented herein by $FXII_{act}$ in the descriptive chemical formula $FXII \xrightarrow{\substack{activator\\surface}} FXII_{act}$. $FXII_{act}$ includes proteins exhibiting either procoagulant potential (protease activity inducing clotting of blood) or amidolytic potential (cleaves amino bonds in s-2302 chromogen but do not cause coagulation of plasma) or both amidolytic potential and procoagulant potential. Apparent yield of procoagulant enzymes was less than purely amidolytic enzymes under all conditions studied. $FXII_{act}$ also includes proteins that remarkably suppress production of procoagulant enzymes but does not suppress production of purely amidolytic enzymes.
6. The relative reactive proportions of proteins subsumed by $FXII_{act}$ were found to depend on activator surface chemistry/energy. Thus, it appears that *FXII* undergoes some kind of chemical

transformation by contact with any kind of activator surface, quite independent of hydrophilicity or surface chemistry; at least in buffer solution.

The *FXII*-derived proteins mentioned in the above item (6) appear to be in a complex statistical ensemble of a large number of states, with some states of low local stability and others with high stability. Phenomena such as allosteric regulation are often ascribed to arise from equilibrium between two major conformations of dynamic proteins [6]. It is not proven herein that *FXII* exists in more than one conformer state, but change in conformation with various perturbants has been observed [7].

Precise biochemical mechanisms for reactions involving *FXII* are not well understood, but in-vitro activation of *FXII* has been variously attributed to proteolytic cleavage[8-14] change in conformation [7, 15-21] or a combination of these mechanisms [10, 22]. Speculation on the nature of these conformation changes is hampered by the fact that 3-D crystal structures of *FXII* and its cleavage products are not clear, with only a few studies conducted using computer models [23].

In light of the above, it has become evident that a molecular inventory of proteins and conformers resulting from *FXII* autoactivation under different experimental conditions with activators spanning a full range of surface chemistry/energy is a necessary step in the formulation of testable mechanisms of autoactivation. In turn, formulation of testable mechanisms is essential to the long-sought ability to prospectively surface engineering cardiovascular biomaterials with improved hemocompatibility. This inventory will complement purely functional assays; hopefully leading to an identification of those specific protein(s) comprising $FXII_{act}$ that is (are) responsible for the above-mentioned amidolytic, procoagulant, and procoagulant-suppressive activity. Present work also sheds light on putative “self reactions” between *FXII* and *αFXIIa* in buffer solution in the absence of activator surfaces (other than that of test tubes and cuvettes in which experimental

solutions are contained). Herein, we report results from a two-prong research strategy using high-resolution electrophoresis coupled with chromogenic and plasma-coagulation functional assays.

4.2.0. Methods and materials

4.2.1. Plasma and coagulation proteins

Citrated human platelet poor plasma (PPP) was prepared from unexpired pooled lots obtained from the M.S. Hershey Medical Center Blood Bank and prepared as described previously [24-26].This work was performed with a single batch of PPP aliquoted into 15 ml polypropylene tubes (Falcon, Becton Dickinson) and frozen at -20 °C until use. Experiments for this work were conducted within a month of PPP preparation. Repeat trials yielded no significant variations in coagulation times within this experimental time frame.

Human *FXII* and *αFXIIa* were used as received from Enzyme Research Laboratories (South Bend, IN). Activity of both *FXII* and *αFXIIa* was specified by the vendor in mg/mL or traditional units of plasma equivalent units per mL (PEU/mL)[27]. Neat-buffer solutions of *FXII* and *αFXIIa* solutions were prepared in phosphate buffer saline (PBS; Sigma; 0.14 m NaCl, 3 mm KCL prepared from powder in 18 mΩ de-ionized water, pH 7.4).

4.2.2. Preparation and characterization of particulate activators

Test activator surfaces used in this work were 425-600 μm diameter glass particles (Sigma Aldrich) in either cleaned or silanized form. The nominal specific area of the glass particles used in this work was 5×10^{-3} m^2/g (based on 512.5 μm mean diameter and 168 μg/particle). The surface

area measured by the Brunauer-Emmett-Teller (BET) method (Micromeritics ASAP 2000 using liquid nitrogen as the probe gas) was (8.5±0.1) $\times 10^{-3}$ m^2/g. Nominal surface area was used throughout this work as a matter of consistency with prior work and in recognition of the fact that surface area did not influence conclusions based on comparisons among experiments described herein using the same source of particulate activator with a fixed specific surface area.

Silanes (used as received from Sigma Aldrich) applied in this work were octadecyltricholorosilane (OTS) and 3-aminopropyltriethoxysilane (APTES). OTS-treated glass particles were coated in a 0.2% solution of 1,1-pentadecaflurooctylmethacrylate in tricholorotrifloroethane ("Nyebar", Nye Lubricants, Fairhaven, MA) by immersion followed by air drying. Glass cover slips (Fisher 22×30×0.1 mm) were subjected to all surface treatments for particles as described above and further below, providing a substrate suitable for reading phosphate buffer saline (PBS, Sigma) contact angles (see schematic of silanes in Appendix D).

Glass particles and cover slips were first cleaned and activated by 30 min immersion in heated piranha solution (30% H_2O_2 in concentrated H_2SO_4 at approximately 80 °C) followed by 3X sequential washes in each of 18 MΩ de-ionized water and 100% ethanol. Piranha-solution oxidized glass was air dried and subsequently oxidized by air-plasma treatment (10 min at 100 W plasma; Herrick, Whippany, NY) of a single layer of particles (or cover slip) held in a 15 mm Pyrex glass Petri dish, directly before use in silanization procedures or blood-plasma coagulation activation measurements. Glass surfaces treated in this manner were found to be fully water wettable and designated "clean glass". Clean glass particles and cover slip samples were silanized by 1.5 h reaction with 5% v/v OTS in chloroform. Silanized samples were 3X rinsed with chloroform before curing in a vacuum oven at 110 °C for 12 h. Cured OTS samples were optionally immersed in Nyebar solution for 10 min and air dried to produce a surface slightly more hydrophobic than rendered by OTS treatment alone (see Table 3.1). APTES silanization was carried out by 20 min reaction of clean glass with 95:5 v/v ethanol-water solution with 5% APTES that had been

hydrolyzed overnight in the ethanol-water mixture before use. APTES treated glass was 3X washed with ethanol and cured overnight in a vacuum oven at 110 °C.

Table 4.1 Protein yields (as measured by automated electrophoresis) following autoactivation of FXII in the presence of HK and PK in pure-buffer solutions.

	S.No.	Trial I		Trial II		Control Solutions		
		Protein molecular weight[a] (kDa)	Protein yield (%)	Protein molecular weight[a] (kDa)	Protein yield (%)		Protein molecular weight[a] (kDa)	Protein yield (%)
Autoactivation test solution	1		27.68	2.56	27.73	(FXII + HK + PK)	27.40	1.26
	2		2.87	30.30	2.36		29.92	2.51
	3		9.47	34.98	8.30		34.72	7.85
	4		5.24	47.35	5.37		46.77	4.42
	5	57.81	33.73	57.80	40.61		57.18	49.38
	6	65.38	2.65	70.06	3.77		81.24	26.20
	7	70.31	4.06	81.86	26.42		95.73	7.92
	8	82.04	25.1	96.68	11.19	FXII	35.24	0.85
	9	97.15	10.61				97.25	98.94
						PK	92.28	19.73
							98.67	80.27
						HK	171.45	100.00
						PK	92.28	19.73

[a] Molecular weight as read from the Experion unit. Degree of glycosylation affects molecular weight measurements in automated electrophoresis (see Section 4.3.1).

PBS (see above) contact angles on glass cover slip witness samples were measured using an automated contact-angle goniometer (First Ten Angstroms Inc., Portsmouth, VA) that employed the captive-drop method of measuring advancing/receding contact angles (see Refs.[28, 29]for a comparison of goniometric techniques and discussion of experimental errors). Contact angles could not be read directly on glass particles but optical microscopy of the shape of the liquid meniscus of particles partly immersed in water on a microscope slide qualitatively confirmed that the treated particles were not different from the cover slip witness samples. Surface chemistry of glass-particle surfaces has been previously assayed via a diffuse reflectance infrared Fourier transform spectroscopy (DRIFT) collected on a Bruker IFS-66/S Tech as described in Ref.[30].

4.2.3. Determine concentration of proteins

An automated electrophoresis system (Experion, Bio-Rad Laboratories, CA) was used to determine potentially involved in autoactivation. The automated electrophoresis system performs electrophoresis of samples within a microfluidic chip. Within each chip, a series of micro-channels connects the sample wells to a separation channel and buffer wells. A set of electrodes in the electrophoresis station applies a voltage across the micro-channels, causing charged molecules in the samples to migrate into and through the separation channel. Samples are run sequentially, with sufficient lag between each run to prevent cross-contamination. For separation, the micro-channels are filled with a proprietary gel-stain solution (GS) that acts as a sieving matrix, and under denaturing conditions, in the presence of lithium dodecyl sulfate (LDS), the sample proteins migrate through the separation channel at a rate based on their molecular weight. Finally, proteins interact with a fluorescent dye during separation and are detected as they pass a laser and photodiode detector (laser-induced fluorescence).

For this work, 10 lane Experion Pro260 chips were used to separate and quantify proteins. The vendor-defined protocol was used for sample preparation and running the electrophoresis. Chips were first primed with 12 µl of a mixture of sieving matrix (gel) and fluorescent dye (stain). Test solutions (4 µl for each supernate) were mixed with Pro260 sample buffer (2 µl for each sample) in 0.5 mL conical microtubes. Control solutions in neat-buffer, along with a vendor-provided protein ladder, were also processed in a similar manner. The protein solutions were denatured by placing the tubes in a water bath at 98 °C for 5 min. The tubes were allowed to cool and later centrifuged for 15 s to collect the condensate. A bolus of 84 µl of 18 MΩ de-ionized water (obtained from a Millipore Simplicity unit) was added to each micro-tube. The primed micro-chip was loaded with 12 µl gel and gel-stain solution in designated wells. 6 µl of each sample, control and protein ladder solution was added to the wells, and loaded into the Experion station. Experion

software plotted the fluorescence intensity vs. time and produced an electropherogram and virtual gel image. In addition, to test solution peaks, electropherograms also featured system peaks (cluster of signals generated by small molecules that interact with LDS micelles = 8.3 kDa), as well as upper (260 kDa) and lower marker (1.2 kDa) peaks.

4.2.4. Autoactivation reactions in buffer solution

Autoactivation of *FXII* in PBS by clean or silanized glass-particle activators was the primary phenomenon studied in this work. *FXII*, as received from the vendor, was diluted 4x in PBS to prepare a solution at a concentration of 0.28 mg/ml. Concentrations ~10x that of physiological concentration were used in electrophoretic studies to ensure optimum resolution of protein fragments formed. *FXII* activation in PBS solution was carried out as previously described [3,5]. Briefly, 200 µl of *FXII* in PBS at 0.28 mg/mL, at room temperature, was brought in contact with a specific weight of test activator (detailed in Sections 4.2.4.1 - 4.2.4.4) for between 5 and 70 min. Supernatant from these experiments were then analyzed by automated electrophoresis as detailed in Section 4.2.3. Each electrophoresis microchip also contained control samples of *FXII* in PBS (0.28 mg/mL) that were not incubated with particulate activators.

4.2.4.1. Surface area titration of purified *FXII* in buffer solution

The autoactivation protocol detailed above was carried out with incrementally varying mass between 0 and 50 ± 0.1 mg (nominal surface area of 5.0×10^{-4} m^2) of clean glass activator weighed using a laboratory electronic balance. Autoactivation was carried out by 30 min contact of 200 µl of *FXII* in PBS at 0.28 mg/mL with clean-glass surfaces in 2 mL microtubes (VWR).

Autoactivation supernate was analyzed using automated electrophoresis as detailed in Section 4.2.3.

4.2.4.2. Autoactivation of *FXII* with procoagulants with varying surface energy

Test solutions of *FXII* were prepared at concentrations of 0.28 mg/mL in 2 mL microtubes (VWR). 200 µl of the solution was incubated with 100 mg of clean glass, APTES-silanized or Nyebar-coated-OTS-silanized glass for 10 min and 70 min. Supernatant from each microtube was evaluated in the Experion automated electrophoresis unit as detailed in Section 4.2.3.

4.2.4.3. Concentration titration of FXII

Test solutions with *FXII* in PBS were prepared at concentrations of 0.28 mg/mL. Three additional concentrations of *FXII* (0.14, 0.07, 0.035 mg/mL) were prepared by 50% serial-dilution. *FXII* solutions at each concentration were incubated with 100 mg of clean-glass activator for 30 min. Test supernatant and *FXII* control at each concentration were then analyzed by the Experion automated electrophoresis unit as described in Section 4.2.3.

4.2.4.4. Kinetics of FXII autoactivation

FXII test-solutions in PBS (200 µl at 0.28 mg/mL) were incubated for durations ranging from 10 min to 70 min with 100 mg of clean-glass activators and silanized particle activators. Test supernatant were then analyzed in the Experion unit as described in Section 4.2.3.

4.2.5. Autoactivation of *FXII* with PK and HMWK

Test solution containing 0.15 mg/mL of *FXII*, 0.20 mg/mL of prekallikrein(*PK*) and 0.43 mg/mL of high-molecular weight kininogen(*HMWK*) was prepared and 3x serially diluted by 50% to prepare four test solutions containing these proteins in molar ratios similar to those found physiologically [1]. 200 µl of the test solutions were incubated with 100 mg of clean glass for 60 min. Supernatant from each microtube was evaluated in the Experion automated electrophoresis unit as detailed in Section 4.2.3. Control solutions containing the above mixture of proteins incubated in the absence of clean-glass activator, and solutions containing each of the reagents individually were also added to the microchip to compare results.

4.2.6. Autohydrolysis reactions in buffer solution

Autohydrolysis reactions were carried out by timed incubation of *FXII* and *αFXIIa* in neat-buffer solutions. 200 µl test solutions containing varied [*αFXIIa*] (0.06, 0.13, 0.20, 0.30, 0.50, 0.75 PEU/ml) and 0.03 mg/ml of *FXII* in PBS, were prepared by gentle pipette aspiration and allowed to stand undisturbed in 0.5 mL conical microtubes (Safe-lock microcentrifuge tubes, Eppendorf) at room temperature for 30 min. Autohydrolysis supernatant was subsequently evaluated by a coagulation time (CT) assay to measure procoagulant activity and a chromogenic assay to measure amidolytic activity using protocols detailed in Ref.[3]. The above protocol was repeated with *FXII* at 0.015 and 0.075 mg/ml, to evaluate the effect of varying *FXII* concentration on autohydrolysis. *FXII* plasma titrations were conducted to determine control CT values. Difference in CT for autohydrolysis supernates and control supernates was calculated as Δ_{CT}. Similarly a difference in absorbance rate (as measured by the UV–Vis Spectrometer) was calculated as $\Delta_{\text{Absorbance Rate}}$.

Electrophoretic identity of autohydrolysis products was established through automated electrophoresis. Serially diluted solutions starting with 0.20 mg/ml each of *FXII* and *αFXIIa* in neat-buffer solution were mixed by gentle pipette aspiration and incubated for 30 min at room temperature. Concentrations ~10x physiological [*FXII*] were used to ensure effective resolution of the *FXII* autohydrolysis suite. Autohydrolysis supernates were then analyzed by an automated-electrophoresis system as detailed in Section 4.2.3.

4.3.0. Results

4.3.1. Electrophoresis of *FXII* and *αFXIIa* reagents

Electrophoresis of *FXII* and *αFXIIa* reagents was carried out in the Experion system as outlined in Section 4.2.3. Experion software plotted the fluorescence intensity vs. time (electropherogram), as shown in Figure 4.1, and generated a virtual gel image. Electrophoresis for both reagents was conducted in reducing, as well as, non-reducing buffer (not shown). As is evident, vendor-sourced *FXII* (Panel B, Figure 4.1) exhibited a single peak at ~82 kDa. Vendor-supplied *αFXIIa* (Panel A, Figure 4.1) exhibited three main peaks at 29, 52 and 58 kDa with <1% of other proteins/contaminants. In addition, to test solution peaks, electropherograms also featured system peaks (cluster of signals generated by small molecules that interact with LDS micelles~8 kDa), as well as upper (260 kDa) and lower marker (1.2 kDa) peaks that were used by the Experion unit to normalize the data.

A ~15-18% higher molecular weight for *FXII* and *αFXIIa* proteins was consistently observed with automated electrophoresis when compared with conventional SDS-PAGE. According to the vendor, this is purportedly due to glycosylation of *FXII* and *αFXIIa* and has been

observed with other glycosylated proteins [31]. Electrophoresis with deglycosylated reagents was not conducted to avoid artifacts. However, molecular weights read from the Experion system, were uniformly scaled down by 15% to avoid confusion and maintain consistency with conventional SDS-PAGE.

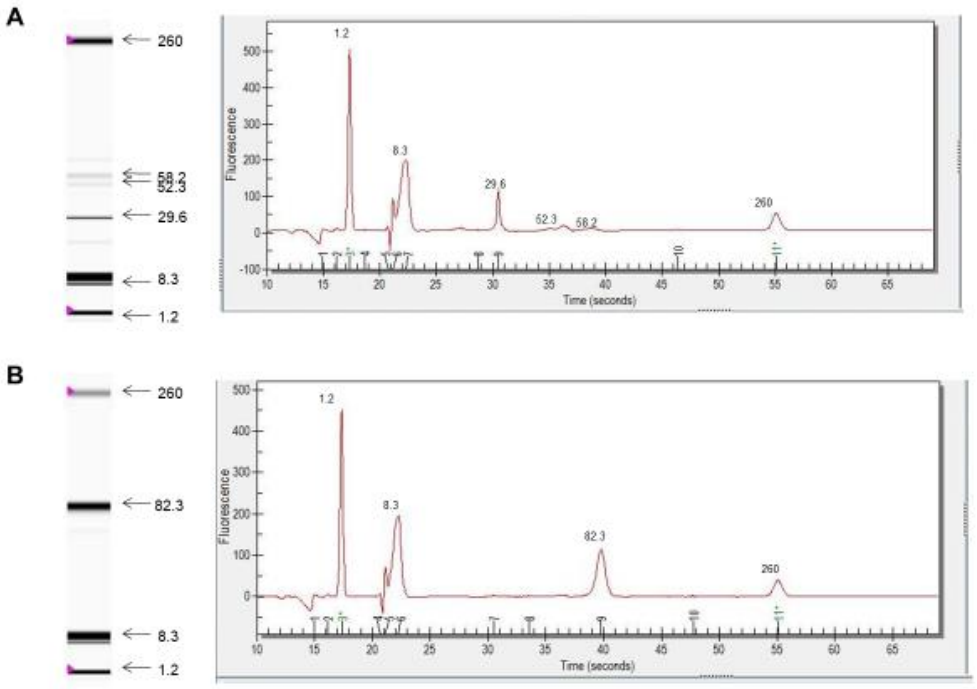

Figure 4.1 Electropherogram and virtual-gel image, in reducing buffer, for *αFXIIa* (Panel A) and *FXII* (Panel B). In addition to test solution peaks, electropherograms and gel-images also feature system peaks (cluster of signals generated by small molecules that interact with LDS micelles ~8.3 kDa), as well as upper (260 kDa) and lower marker (1.2 kDa) peaks that normalize the data.

4.3.2. Autoactivation as a function of procoagulant surface energy

Products of *FXII* autoactivation with clean-glass and silanized-glass activators were analyzed in reducing buffer using the Experion automated electrophoresis system as detailed in Section 4.2.3. Figure 4.2A is the virtual-gel image generated by the instrument. Upper and lower

bands at 260 kDa and 1.2 kDa are present in the vendor-provided buffer, and the band at 8.3 kDa is system generated. The only band visible from test-solutions was found to be at ~80 kDa for activation supernatants from both clean-glass and silanized-glass activators. Proteins in this band accounted for >99% of the autoactivation supernatant. Figure 4.2 B plots the concentration of all protein fragments as measured by the Experion system. Concentration of the 80 kDa fragment, in the case of clean-glass and Nyebar autoactivation, appeared marginally lower than that for *FXII* control. However, the percentage of total for the 80 kDa band (output provided by the Experion system) in all test-solutions was >99%, and differences appeared to be due to error in loading proteins. The other band observed in some test samples was ~29 kDa (<0.001 mg/ml). However, this was found in similar low concentrations within *FXII*-control samples as well, and deemed to be an unknown contaminant.

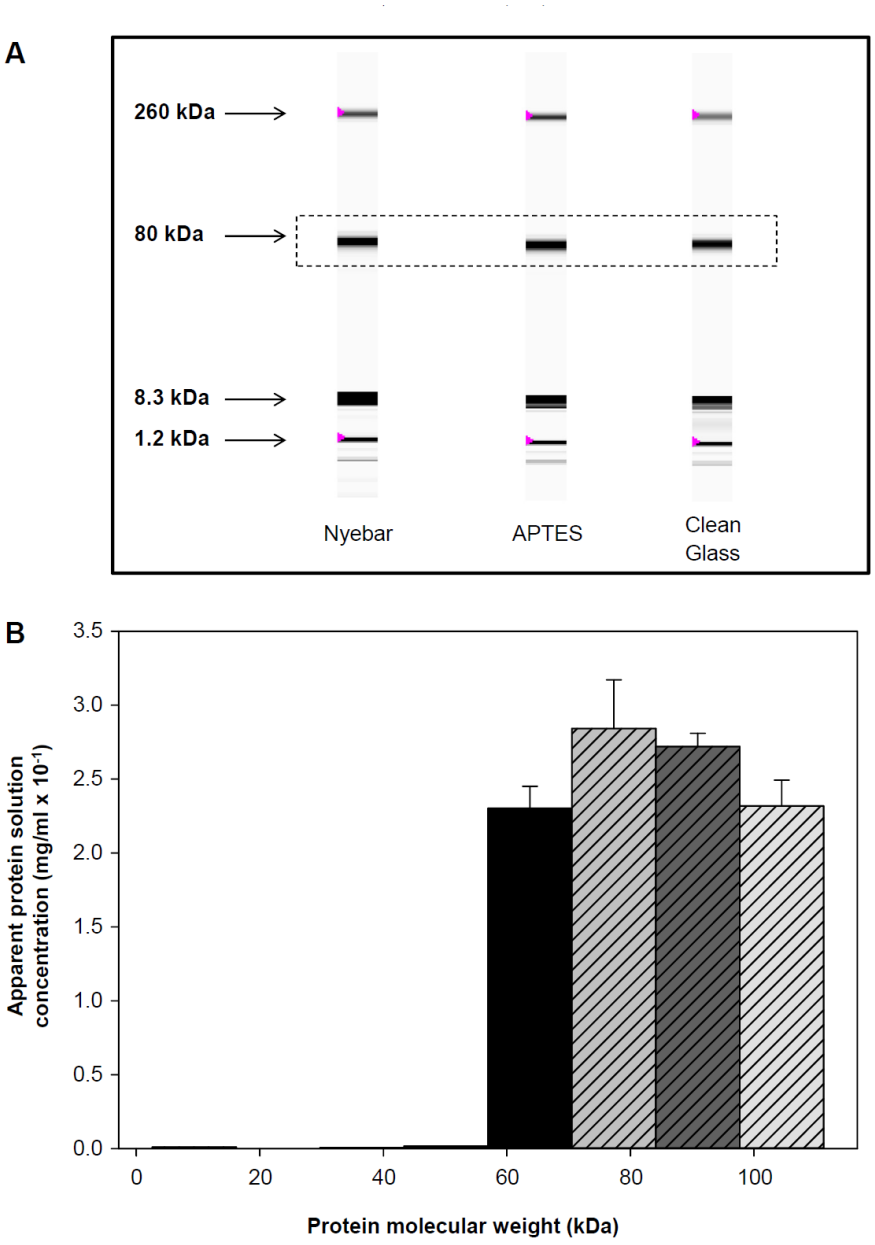

Figure 4.2 Autoactivation as a function of procoagulant surface energy. Panel A shows virtual gel images of autoactivation supernatant in reducing buffer, obtained by contacting neat buffer solutions of *FXII* (0.28 mg/ml) with clean-glass and silanized-glass activators, for 70 min. The only band visible is at ~80 kDa which represents >99% of autoactivation product in all three experiments. Panel B plots the concentrations of these proteins (medium grey: APTES; dark grey: clean glass; solid black: Nyebar) in comparison to *FXII* control (light grey). Data and error bars represent mean and standard deviation of N = 2 measurements. A marginally lower concentration of the 80-kDa fragment was observed in case of clean glass and Nyebar activator particles, however there was no concomitant increase in other protein fragments, and 80 kDa protein yield in all cases was ~99%. Evidence of proteolysis was thus not seen with clean and silanized glass activators.

4.3.3. Effect of varying experimental parameters (clean glass activator surface area, FXII concentration and incubation time) on autoactivation

Figure. 4.3 illustrates the percentage of 80 kDa protein in total autoactivation-supernatant, as a function of clean-glass activator surface area. Apparent yields following autoactivation were close to 100% and not statistically distinct from those in pure-buffer solutions of *FXII*. No evidence of *FXII* proteolysis was thus observed by varying clean-glass activator surface area.

Continuous incubation with clean-glass and silanized particle activators exhibited a similar trend (not shown). The 80 kDa band did not exhibit a statistically significant change in concentration even after 70 min of continuous incubation of *FXII* solution with clean glass and silanized particle activators. The ~80 kDa band represented >99% of the autoactivation suite, and the concentration of the other minor fragments/contaminants in test-solutions (<1%; not shown) was not significantly different than concentration in control solutions of *FXII*.

Apparent concentrations of the 80 kDa protein in total autoactivation-supernatant, as a function of *FXII* solution concentration (not shown) were within in the 98–100% range and were statistically indistinguishable from those in pure-buffer solutions of *FXII*.

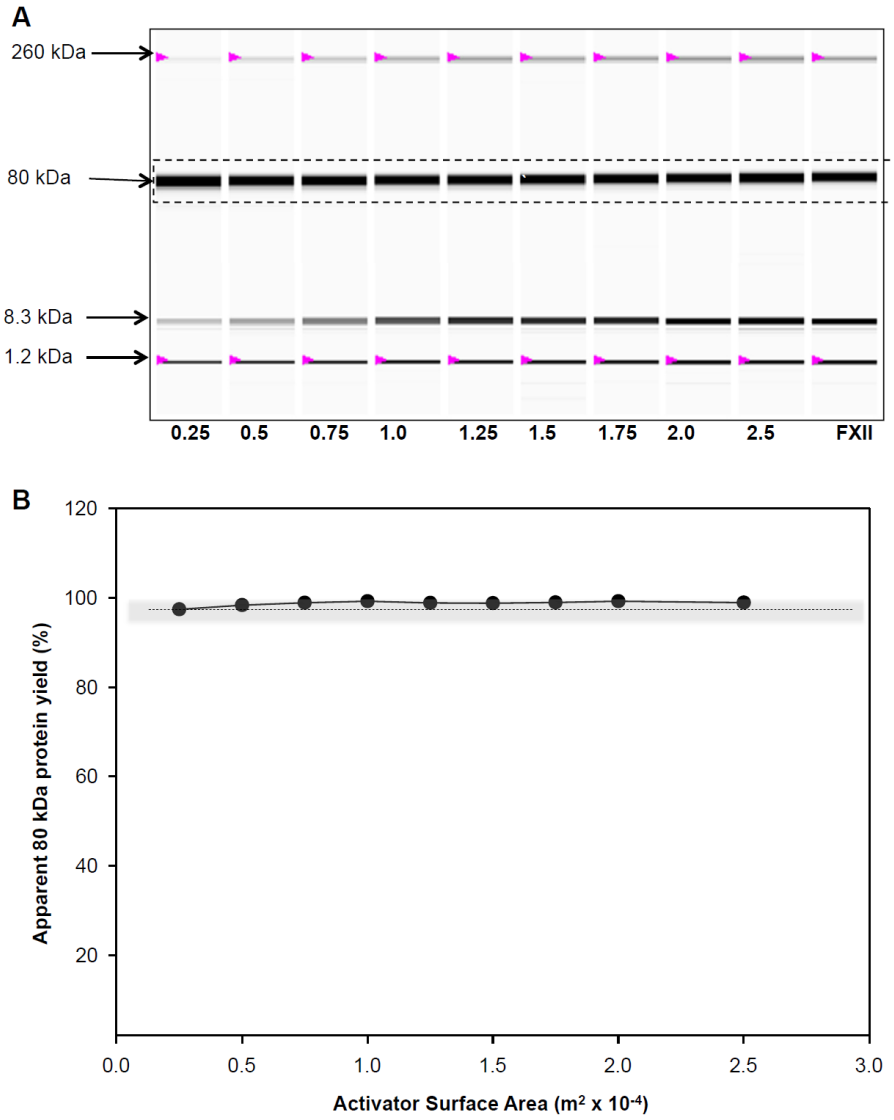

Figure 4.3 Surface-area dependence of *FXII* autoactivation in buffer solution. Panel B plots the percentage of the 80 kDa fragment in autoactivation supernatant, produced with varying surface-area of clean-glass activator. Dashed line and grey area shows mean and standard deviation of the 80 kDa fragment in 0.28 mg/mL FXII control. There was no dependence on activator surface area, and no significant difference in the percentage of the 80 kDa fragment appeared on autoactivation when compared to *FXII* control. Bands suggestive of the formation of *αFXIIa* or *βFXIIa* did not appear at clean-glass activator surface areas used in this study. Panel A is the corresponding virtual gel image generated by the Experion automated electrophoresis unit.

4.3.4. FXII contact activation in the presence of PK and HMWK

To simulate reciprocal-activation *in vitro*, we used an experimental environment that included *FXII*, high-molecular weight kininogen (*HMWK*) and prekallikrein (*PK*) in PBS incubated with clean-glass activators. This system was simplistic owing to the absence of other substrates and inhibitors for each reagent, but offered an incremental increase in biochemical complexity compared to *FXII* autoactivation studies in buffer without exogenous proteins and had the advantage of easy analysis by electrophoresis.

Products of *FXII* autoactivation with clean-glass in the presence of *HMWK* and *PK* in PBS were analyzed using the Experion automated electrophoresis system as detailed in Section 4.2.3. Figure 4.4 (Test) presents the virtual-gel image generated by the instrument for autoactivation with clean-glass whereas Figure 4.4 (Control) has the virtual-gel image for a mixture of the reagents incubated without clean-glass. The image in the upper-left box is the virtual-gel for individual reagents. Upper and lower bands at 260 kDa and 1.2 kDa are present in the vendor-provided buffer and the band at 8.3 kDa is system generated. A 15–25% higher molecular weight for reagents, test and control proteins, was reported by the instrument purportedly due to glycosylation of proteins. We did not scale down this data because it was difficult to determine the sources of cleavage fragments and the degree of glycosylation appropriate to each band. Table 4.1 summarizes data from contact-activation and control-solution yields (as read from the Experion unit). Evidence suggestive of proteolysis was found in both the test and control data, even though the correct identity of each protein band could not be ascertained due the impact of glycosylation.

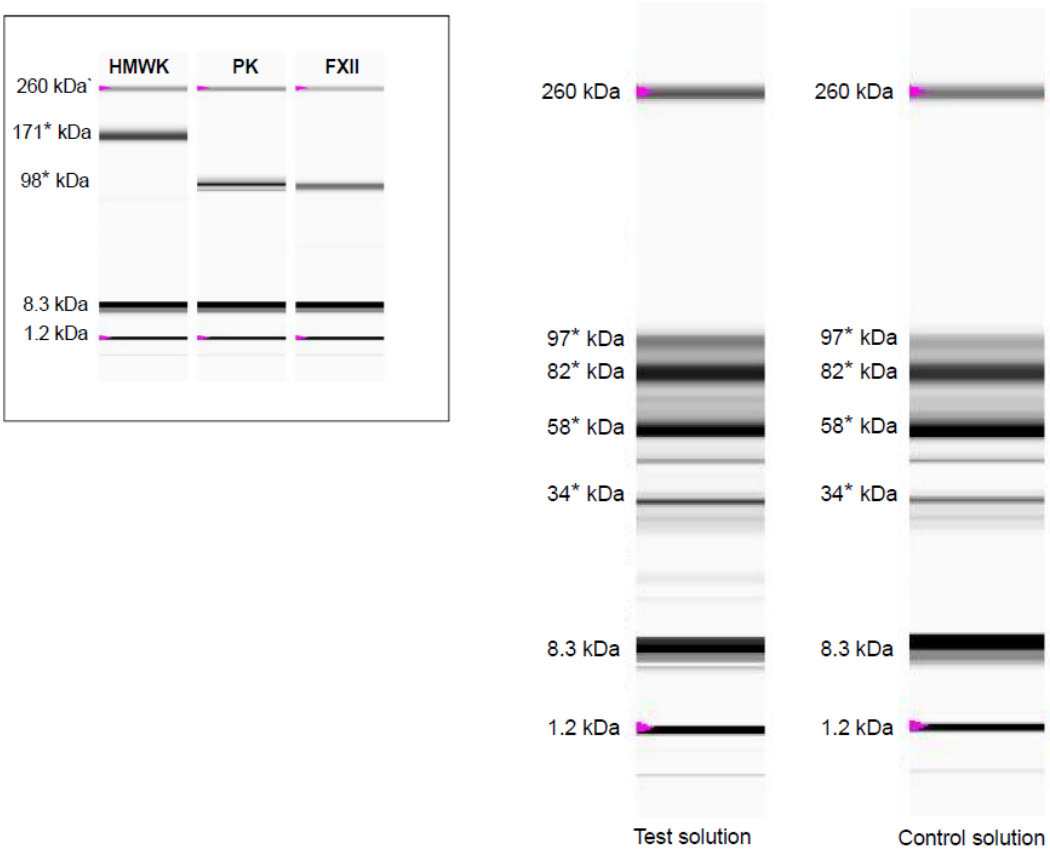

Figure 4.4 *FXII* contact-activation in the presence of prekallikrein and high-molecular weight kininogen. Asterisk (*) indicates that molecular weight measurements for this experiment are as read from the Experion system and not scaled down as for other figures. Test and Control solutions show protein bands <80 kDa which indicate proteolysis in both solutions. Inset shows virtual gel images for Prekallikrein, High-molecular weight Kininogen and *FXII* in PBS as measured separately by the Experion system. Gel-images also feature system peaks (cluster of signals generated by small molecules that interact with LDS micelles ~8.3 kDa), as well as upper (260 kDa) and lower marker (1.2 kDa) peaks that normalize the data.

4.3.5. Plasma coagulation assay for procoagulant activity in autohydrolysis supernate

Increasing concentrations of *αFXIIa*, ranging from 0.06 PEU/ml to 0.75 PEU/ml were incubated with 0.03 mg/ml of *FXII* for time ranging from 2 min to 30 min. Autohydrolysis supernates were then assessed in a CT assay (Section 4.2.6). Using this assay, it was found that the autohydrolysis reaction was effectively instantaneous within the minimum elapsed-time resolution of the experiment (about 2 min) and exhibited no statistically-significant trend over 30 min of testing (not shown).

Average coagulation times (CT) for autohydrolysis supernates, were compared to coagulation times (CT) for an *αFXIIa* titration of plasma. For each concentration of *αFXIIa*, the difference in coagulation time between the experiment and control was calculated as Δ_{CT}. Figure 3.5 (inset) shows that Δ_{CT} scales in an exponential-like manner with *αFXIIa* concentration (best fit line through the data). Whereas the difference Δ_{CT} is ∼6 min at a concentration of 0.06 PEU/ml of *αFXIIa*, an asymptote plateaus to ∼2 min is obtained with increasing concentrations of *αFXIIa*. Furthermore, as is evident in Figure 4.5, the plot of Δ_{CT}/[*αFXIIa*] reveals an exponential decrease, reaching a plateau at ∼3 min per-unit [*αFXIIa*]. Data was fit to $\Delta_{CT} = c+ae^{-b[\alpha FXIIa]}$ by non-linear regression, with c = 1.81±2.65, a = 183.4±19.4, b = 11.9±1.5; $R^2 = 0.99$.

As illustrated in Figure 4.6, Δ_{CT} increases as the concentration of *FXII* increases. While no consistent trend was observed for Δ_{CT}, an exponential decrease in Δ_{CT} per-unit [*αFXIIa*] was observed for all three [*FXII*] tested. Data was fit to $\Delta_{CT} = c + ae^{-b[\alpha FxIIa]}$ by non-linear regression, c = 10.0±2.3, a = 164.7±10.7, b = 9.2±0.9, $R^2 = 0.99$ for autohydrolysis with [FXII] = 0.07 mg/ml; c = 3.9±2.5, a = 205.8±18.8, b = 12.0±1.3, $R^2 = 0.99$ for autohydrolysis with [FXII] = 0.03 mg/ml; c = 3.6±1.6, a = 205.9 ±15.1, b = 13.6±1.1, $R^2 = 0.99$ for autohydrolysis with [FXII] = 0.015 mg/ml.

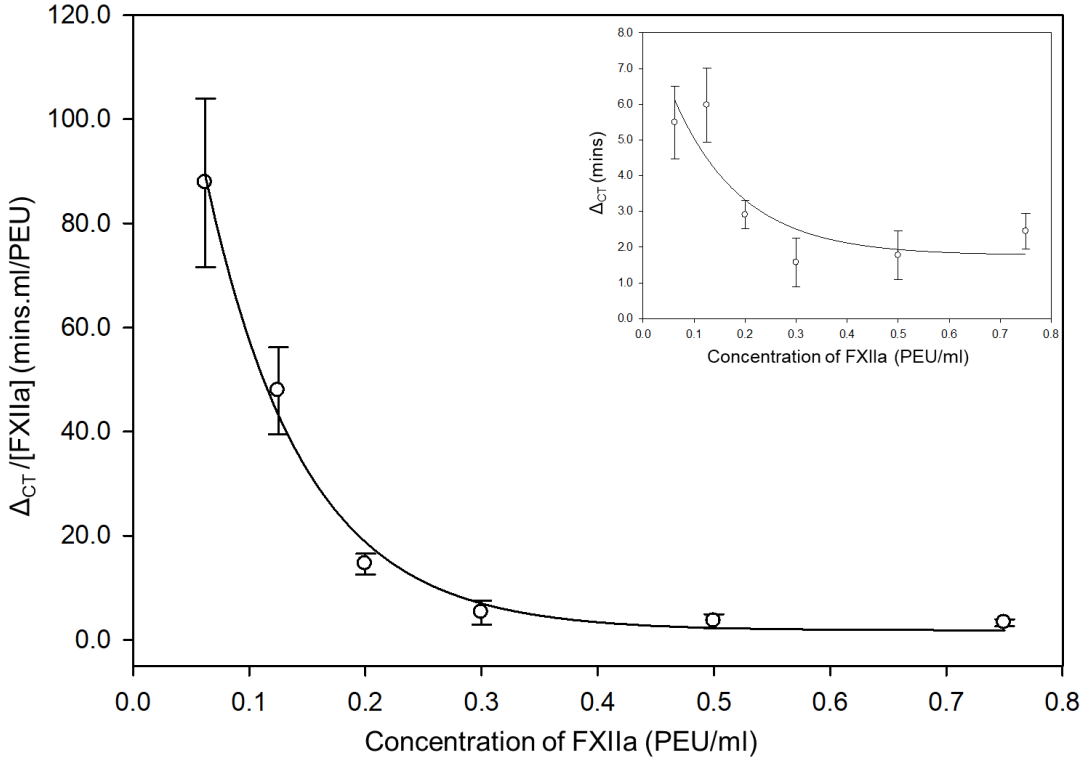

Figure 4.5 Increase in coagulation time (CT) following autohydrolysis in pure-buffer. For each concentration of *αFXIIa*, the difference in coagulation time for autohydrolysis supernate and *αFXIIa* was calculated as Δ_{CT}. Figure. 4.5 (inset) illustrates that the difference in CT scales in an exponential-like manner with *αFXIIa* concentration. While the difference is ~6 min at a concentration of 0.06 PEU/ml of *αFXIIa*, it plateaus to ~2 min at higher concentrations of *αFXIIa*. A plot of Δ_{CT}/[αFXIIa] reveals an exponential trend, plateauing at ~3 min per unit αFXIIa. Data points and error bars represent mean and standard deviation of n = 3 trials. Solid lines through data are best-fit lines obtained by non-linear regression.

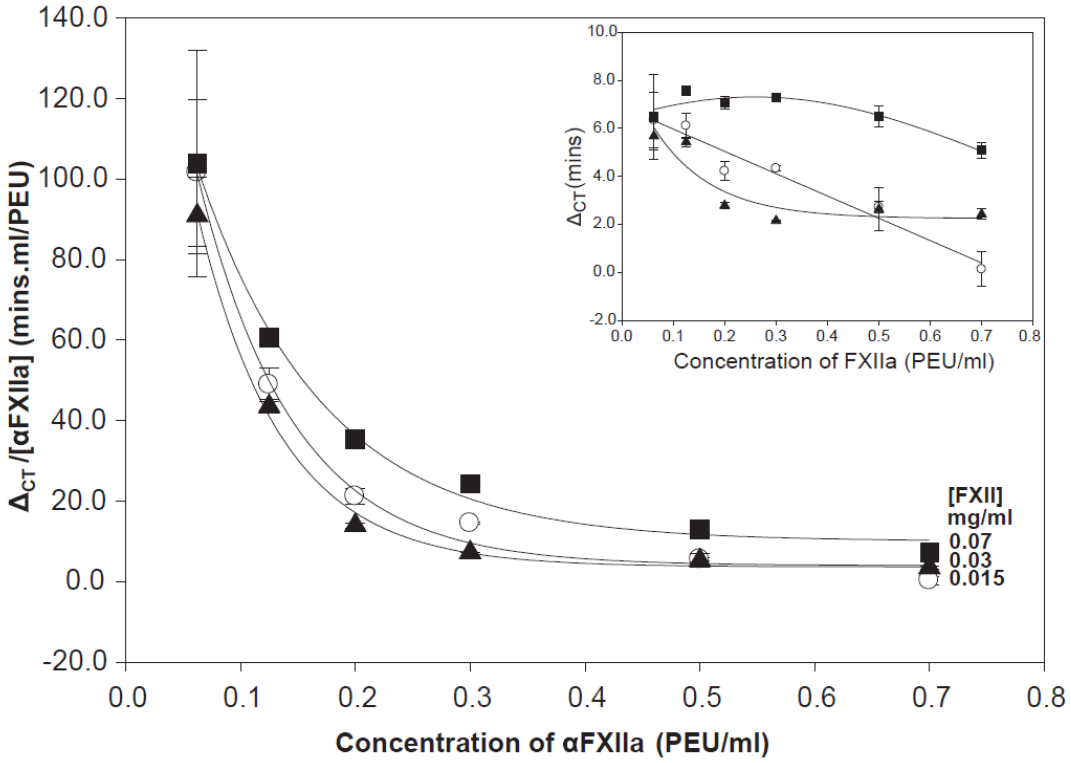

Figure 4.6 Decrease in net procoagulant activity with increasing *FXII* solution concentration. Δ_{CT}/[αFXIIa] increases with increasing *FXII* concentration, where Δ_{CT} is the increase in coagulation time observed upon autohydrolysis, in comparison to αFXIIa alone, as measured by a coagulation time (CT) assay. No consistent trends were observed for Δ_{CT} as a function of *αFXIIa* (inset), however the decrease in procoagulant activity with increasing *FXII* is evident. Solid triangles, open circles, and solid squares correspond to [FXII] at 0.015, 0.03 and 0.07 mg/ml respectively. Data points and error bars represent mean and standard deviation of n = 3 trials. Solid lines through data are best-fit lines obtained by non-linear regression.

4.3.6. Chromogenic assay for amidolytic activity

Average absorbance rates for autohydrolysis supernates, were compared to absorbance rates for *αFXIIa*. For each [*αFXIIa*], the difference in absorbance rates between the two was calculated as $\Delta_{\text{Absorbance Rate}}$. Figure 3.7 (inset) illustrates that the absorbance rates of autohydrolysis supernatant with *FXII* at 0.07 mg/ml and 0.03 mg/ml were higher than control values with *αFXIIa* alone. $\Delta_{\text{Absorbance Rate}}$ also decreases in a linear manner with *αFXIIa* concentration.

A plot of $\Delta_{\text{Absorbance Rate}}/[\alpha FXIIa]$ exhibited an exponential decrease in these two cases. However, autohydrolysis with 0.015 mg/ml of [*FXII*] yielded similar-to-low absorbance rates as compared to *αFXIIa* alone, quite possibly representing threshold values for autohydrolysis products.

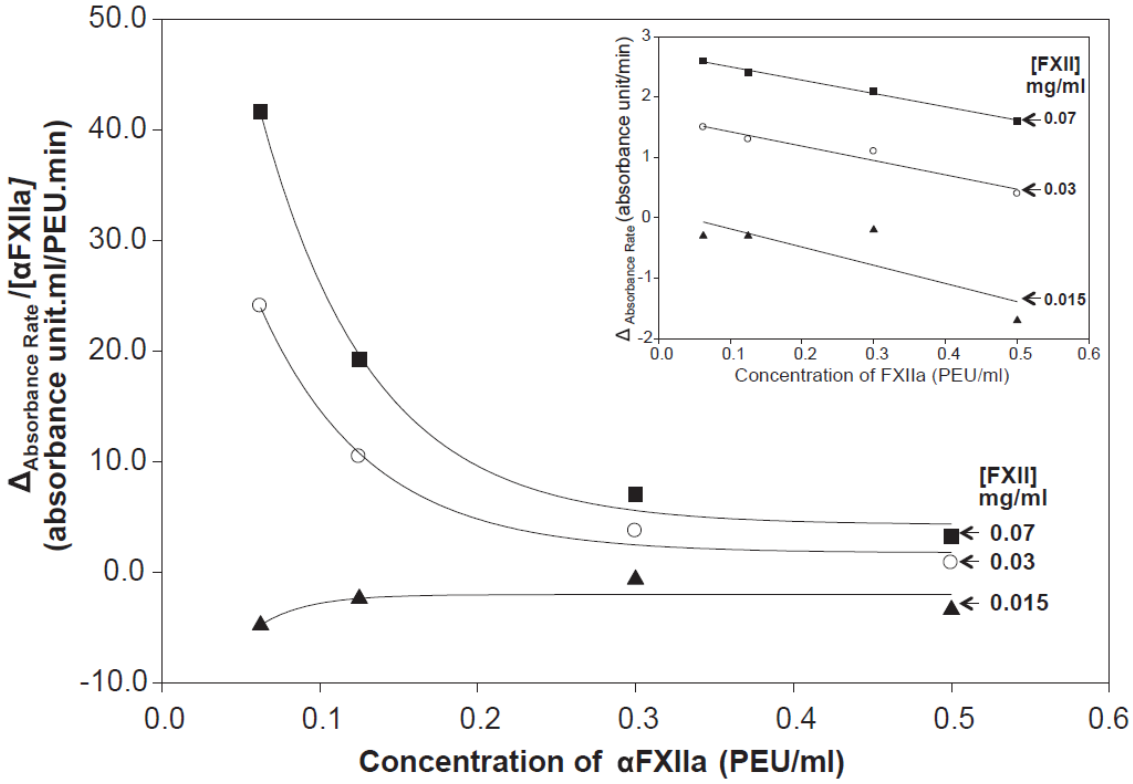

Figure 4.7 Average Absorbance rates for autohydrolysis supernates, compared to absorbance rates for *αFXIIa*. $\Delta_{\text{Absorbance rate}}$ (inset) represents the difference in absorbance rates. $\Delta_{\text{Absorbance rate}}$ decreases linearly with *αFXIIa* concentration while $\Delta_{\text{Absorbance rate}}$ /[αFXIIa] exhibits an exponential decrease. Autohydrolysis with 0.015 mg/ml of *FXII* yielded similar to-lower absorbance rates when compared to [αFXIIa]. ΔAbsorbance rate values were therefore negative. Solid squares represent *FXII* = 0.07 mg/ml, empty circles represent *FXII* = 0.03 mg/ml, and solid triangles represent *FXII* = 0.015 mg/ml. Solid lines are best fit to data.

4.3.7. Electrophoresis of autohydrolysis products

Figure 4.8 illustrates the electrophoretic identity of autohydrolysis products measured in reducing buffer (scaled down by 15%). The molecular suite of autohydrolysis proteins matches closely with the suite observed for the reagents. A comparison in concentration for each of these fragments reveals that with the exception of the 58 kDa fragment, concentrations of other fragments were not statistically different. Solid black bars establish electrophoretic identity of the autohydrolysis proteins, whereas grey bars represent the electrophoretic identity of reagents. The 58 kDa fragment was approximately 50% higher in concentration after hydrolysis. However, no concomitant decrease in concentration for any other fragment, which could account for the appearance of the 58 kDa fragment after autohydrolysis, was observed.

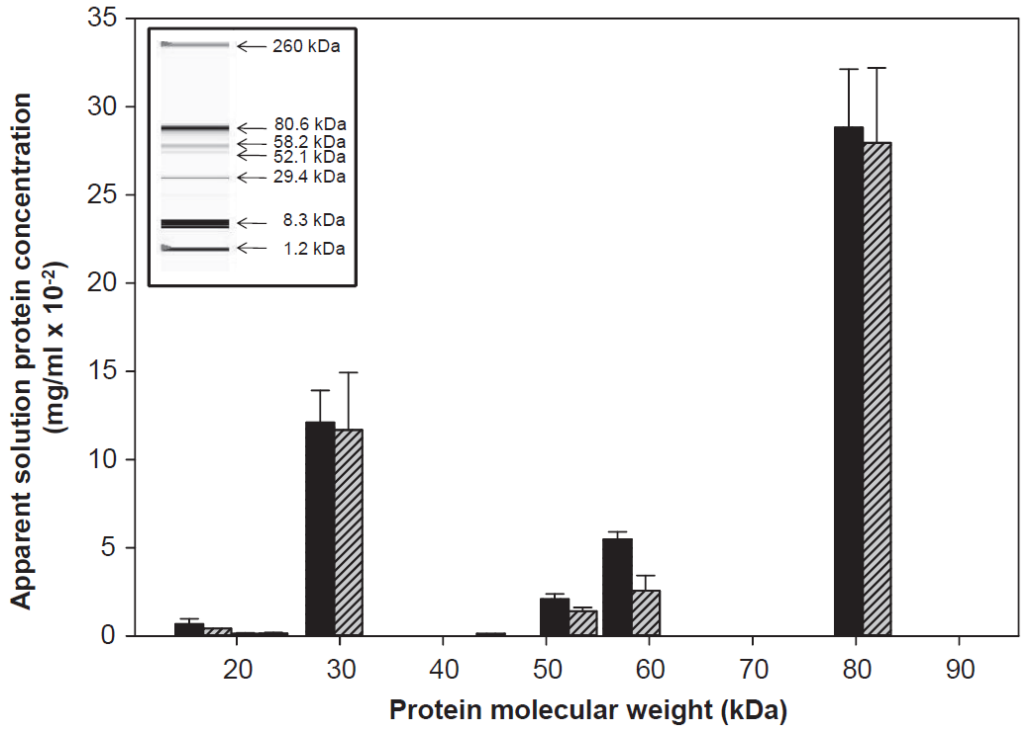

Figure 4.8 Comparison of protein fragments formed with autohydrolysis to those in *FXII* and *αFXIIa* reagents. Solid black bars represent autohydrolysis protein electrophoresis suite, while grey bars represent reagent electrophoresis suite. Data points and error bars are mean and standard deviation for n = 5 measurements. No statistically significant difference is noted.

4.4.0 Discussion

At least three distinct reactions for *FXII* have been described in hematology literature.

1. *Autoactivation*, represented as $FXII \xrightarrow{\substack{activator \\ surface}} FXII_{act}$ takes place when *FXII* comes in 'contact' with an activating surface [1, 10, 15, 32, 33] . While *αFXIIa* and *βFXIIa* are relatively well-known products of autoactivation, the possibility of the formation of minor fragments has been suggested[9, 34]. Oscar Ratnoff also described a single-chain-activated Hageman factor, formed by the incubation of *FXII* with sephadex-ellagic acid [20, 35, 36]. The conformer (termed HF_{ea} exhibited amidolytic potential, but showed no evidence of proteolytic scission when visualized by gel electrophoresis. Thus, autoactivation may be more accurately represented as $FXII \xrightarrow{\substack{activator \\ surface}} FXII_{act}$ source, where $FXII_{act}$ subsumes all FXII autoactivation products including protein fragments and conformers (see Section 4.4.1).
2. *FXII* is cleaved by kallikrein, in plasma, which presumably can be generated by $FXII_{act}$ -mediated hydrolysis of prekallikrein [8, 21, 37]. This mutual activation of prekallikrein and *FXII* is referred to as reciprocal activation. Reciprocal activation accounts for 75% of the $FXII_{act}$ generated in plasma [38].
3. Autohydrolysis of *FXII* is a putative "self-reaction", where *FXII* is a substrate for the *FXII* enzyme. Mathematical models of the intrinsic pathway of blood-plasma coagulation suggest that autohydrolysis is an insignificant reaction in plasma, but significant in pure buffer solutions of *FXII* and *αFXIIa* [26, 38]. Autoamplification appears to be a particular type of autohydrolysis reaction that presumably generates *αFXIIa* by reaction of *αFXIIa* with *FXII*, as described by the chemical formula $FXII + FXIIa \xrightarrow{\substack{activator \\ surface}} 2FXIIa$. Autoamplification has been discussed in past literature (see Ref.[39] and citations therein)

and, in particular, has been proposed to account for differences between chromogenic and plasma-coagulation assays for αFXIIa in buffer solution [39]. Subsequent work [3, 5]casts doubt on this latter proposal, suggesting instead that a less specific autohydrolysis reaction of the type $FXII + FXIIa \xrightarrow{\substack{activator \\ surface}} amidolytic\ protein$ accounts for the discrepancy between chromogenic and plasma coagulation.

Prekallikrein is a zymogen composed of two molecular-weight-variants of a single polypeptide chain: 88 kDa and 85 kDa. Following reciprocal activation, prekallikrein is converted to kallikrein, which consists of a heavy chain (52 kDa) linked by disulfide bonds to a light chain of either 36 kDa or 33 kDa. A variant called β-kallikrein has a cleaved heavy chain broken down into molecular weights of 28 kDa and 22 kDa. Kallikrein has a wide variety of substrates in plasma in addition to Factor XII which include high-molecular weight kininogen (*HMWK*), plasminogen, C3 and prorenin. C1 inhibitor and α2 macroglobulin account for over 90% of the inhibitory activity of kallikrein in normal plasma[40]. *FXII* activates to form *αFXIIa* by cleaving the bond connecting Arg353–Val354 and generating a two-chain molecule composed of a heavy chain 52 kDa and a light chain 28 kDa, held together by a disulfide bond. Proteolytic cleavage further proceeds on αFXIIa to yield a major active product at a molecular weight of 40 kDa, as well as *βFXIIa*, which appears as two closely related molecular species of molecular weight 28 kDa and 30 kDa. A minor active product of molecular weight at 70 kDa is also observed. Other minor fragments of *FXII* have also been hypothesized as well as observed [3]. The *FXII* suite is inhibited by C1–INH, α2-antiplasmin, α2-macroglobulin and antithrombin III.

Changes in conformation accompanying activation of purified *FXII* were first studied by Revak and Cochrane [8, 21]. They found that activation of purified Hageman factor with negatively

charged surfaces (so-called ‘solid phase activation’) resulted in a putative conformational change in the molecule, while activation with kallikrein and plasmin caused proteolytic cleavage [41-43].

McMillin *et al*. [7, 17] and Samuel *et al*. [16, 19] used circular-dichroism spectroscopy to observe changes in conformation following activation of *FXII*. Samuel et al. further proposed that activation with dextran sulfate was biphasic, with a first rapid phase associated with small but significant changes in protein secondary structures, followed by a second slow phase of proteolytic cleavage also accompanied with changes in conformation. Oscar Ratnoff too observed that *FXII* exposed to sephadex-ellagic acid in the absence of proteolytic agents exhibited amidolytic activity, but had not undergone scission [20], leading him to conclude that chain-scission may not be necessary for clot-promoting properties of *FXII* in plasma. He called this single-chain activated form ‘HFea’ [35, 36, 44]. Later Heimark et al. [45] proposed a tentative mechanism for the surface activation of blood coagulation with kaolin which suggested that the initial event in the activation of blood coagulation involves a substrate-induced catalysis by single-chain *FXII* ‘bound’ to kaolin, suggesting that kaolin-activated single-chain *FXII* has sufficient enzymic activity to propagate the intrinsic cascade. Finally, Citarella et al. [46] summarized two views of the idea that change in conformation of *FXI in vitro* (see Ref. [46] and citations therein) led to activation. The ‘autoactivation’ hypothesis, postulates that binding of *FXII* to a negatively charged surface induces conformational changes in *FXII*, and is the key event that initiates autoactivation. An alternate ‘susceptibility’ hypothesis states that *FXII* bound to a surface does not autoactivate but rather undergoes a conformational change that enhances its susceptibility for cleavage by kallikrein.

4.4.1. FXII contact-activation in the absence of plasma proteins

Experimental evidence discussed in Sections 4.3.2 and 4.3.3 using high-resolution electrophoresis, indicates that *FXII* does not undergo proteolytic cleavage following autoactivation with clean-glass and silanized-glass activators in the absence of plasma proteins. However, given that procoagulant and amidolytic activity have been observed and quantified previously under similar in-vitro experimental conditions [3, 47], we are led to hypothesize, but not yet finally conclude that *FXII* undergoes changes in conformation following contact-activation with an activator surface (irrespective of its surface energy or chemistry), in the absence of plasma proteins, as hypothesized by earlier studies. Section 4.3.3 indicates that conformer formation exhibits no measurable kinetics and does not depend upon activator surface-area or *FXII* concentration. It is not certain whether all available *FXII* is converted into active conformers. The self-limiting nature of autoactivation, along with low yields of the autoactivation suite (<10%) as measured by chromogenic and plasma coagulation assay seem to indicate either partial conversion of *FXII* into conformers, or weak procoagulant and amidolytic potential of conformers.

Moreover, as described in Section 4.3.1, conformer activity varies with surface chemistry/energy of activator surfaces. We cannot speculate based on this work, on the nature of changes that take place in the 3-D conformation of the *FXII* molecule, but evidence presented herein seems to suggest that *FXII* can indeed exist in more than one conformer state, possibly depending on vicinal water properties [48] (here “vicinal water refers to the interfacial aqueous phase separating the physical surface from the bulk solution that is hypothesized to have different properties than the solution.

4.4.2. *FXII* contact-activation in the presence of prekallikrein and high molecular-weight kininogen

Products of *FXII* contact-activation with clean-glass in the presence of high-molecular weight kininogen (*HMWK*) and prekallikrein (*PK*) in PBS differed significantly from those in case of *FXII* contact-activation in the absence of proteins. In this experiment, evidence of proteolysis was apparent in both experiment and control vials as these showed multiple protein bands with molecular weight <80 kDa. Proteolytic fragments with average molecular weights of ~58 kDa (as read from Experion unit and not corrected for error due to glycosylation) constituted the highest percentage in the suite (see Table 4.1). It is important to note that the distribution of fragments was similar in both experiments (with clean-glass activator) and control (without clean-glass activator surface) and could be due to the presence of minor concentrations of either *αFXIIa* or Kallikrein, which trigger the reciprocal activation pathway. Alternatively, since *FXII* autoactivation, and subsequent conformer formation, does not exhibit surface area dependence and is efficient even with hydrophobic surfaces, the small surface area of polystyrene test-tubes might have been sufficient to produce small quantities of *FXII* conformers which in turn trigger the reciprocal-activation route. This finding seems to support earlier results by Kaushik *et al.* [24] which indicated that prekallikrein hydrolysis is not localized to an activation complex on the procoagulant surface [24]. Either scenario is indicative of the importance of reciprocal-activation and its role as the major *αFXIIa* generator as shown previously [38].

The protocol used for this experiment, while simplistic does indicate significant potential in a systematic analysis of contact-activation of *FXII* in the presence of plasma proteins.

4.4.3. Procoagulant activity following autohydrolysis in buffer solution

As is evident from Figure 4.5 and Figure 4.6, autohydrolysis does not lead to production of proteins with procoagulant activity, where activity is measured in terms of plasma coagulation time (CT). Whereas this functional assay does not identify the number or kind of proteolytic proteins produced by autohydrolysis, and proteolytic activity does not in itself measure concentrations of putative protein fragments/conformers, the measurable decrease in coagulation time is evidence for to the formation of proteins that directly affect *αFXIIa* procoagulant activity, or procoagulant-stimulus transmission down the cascade.

Whereas the specific biochemical mechanism for autohydrolysis remains open to speculation, possible mechanisms can involve the *FXII* molecule itself (i.e. denaturation or changes in conformation of *αFXIIa*) that render it less effective; action of *αFXIIa* on target-proteins (i.e. blockage/inhibition of proteolytic cleavage of *FXI* and prekallikrein; or other components of the cascade downstream that influence the coagulation time CT). It is reasonable to speculate that the cause of the aforementioned effects is (are) either protein fragments, conformers of *FXII* and/or *αFXIIa*, or complexes of these two proteins. Inhibition is maximal at lower concentrations of *αFXIIa* and plateaus to a minimum of ∼2 min as [*αFXIIa*] increases. This is possibly because at higher [*αFXIIa*], procoagulant stimulus >> threshold value required for sufficient fibrin formation. Hence even if a small portion of *αFXIIa* is inhibited, the final effect would be much less pronounced. Increasing [*FXII*] leads to an increase in Δ_{CT} and Δ_{CT}/[*αFXIIa*] as shown in Figure 4.6, pointing to a direct increase in autohydrolysis products with an increasing [*FXII*].

4.4.4. Amidolytic activity following autohydrolysis in buffer solutions

Figure. 4.7 illustrates that $\Delta_{\text{Absorbance rate}}$ decreases in a linear manner with increasing *αFXIIa*. The decrease is linear rather than asymptotic (as in plasma) most likely because the PBS/chromogen system does not suffer from stimulus-processing limitations as in human plasma [5].

These results along with that of Section 4.4.2, point to the formation of *FXII*-derivative proteins that have amidolytic activity, but not procoagulant activity. These proteins may possibly be similar to $FXII_{act}$ proteins which exhibit amidolytic activity but not procoagulant activity, and additionally have activation-suppressing potential [3].

4.4.5. Electrophoretic identity of autohydrolysis products

Figure. 4.1, Figure. 4.8 illustrate the electrophoretic identity of reagents (*FXII* and *αFXIIa*) and autohydrolysis proteins respectively. A careful comparison of the electrophoretic-fragment profile in the two figures reveals little evidence of proteolytic cleavage following autohydrolysis. Moreover, a systematic comparison of fragment concentrations revealed that most protein fragment concentrations for autohydrolysis were not statistically different from a simple sum of the reagents. We did observe an isolated increase in the 58 kDa fragment following autohydrolysis, but did not see a concomitant change in any other band. The differences between the two could thus be due to experimental differences in amount of protein loaded and assayed.

We are thus led to hypothesize, but not conclude, that autohydrolysis leads to the formation of conformers of *FXII* that have amidolytic activity but no procoagulant activity. We cannot prove or disprove the possibility of the formation of additional conformers with neither amidolytic nor

procoagulant activities that inhibit *αFXIIa* procoagulant stimulus and transmission down the cascade.

4.5.0. Conclusions

High-resolution electrophoresis of *FXII* autoactivation proteins in neat-buffer solution does not show bands indicative of proteolytic fragment formation. Change in experimental parameters such as activator-surface area, activator surface-energy, *FXII* solution concentration and incubation time did not lead to formation of either *αFXIIa* or *βFXIIa* as evidenced by automated electrophoresis. Correlating this with previous experimental findings which indicate that *FXII* autoactivation in the absence of plasma proteins creates proteins that exhibit procoagulant and/or amidolytic potential, the relative proportions of which depend on activator surface chemistry/energy, we are led to hypothesize that autoactivation creates an ensemble of single-chain active *FXII* conformers. These conformers may possibly be an intermediate step in the contact-activation reactions as they undergo proteolytic cleavage in the presence of prekallikrein and high-molecular weight kininogen, as suggested by earlier investigators. Furthermore, we have found that net procoagulant activity (protease activity inducing clotting of plasma) measured by a plasma-coagulation assay, decreases systematically with increasing *FXII* solution concentration. This implies that *αFXIIa* activity is inhibited by an unknown reaction between *FXII* and *αFXIIa*. Under the same reaction conditions, chromogenic assay reveals that net amidolytic activity (cleavage of amino acid bonds in s-2302 chromogen) increases with increasing *FXII* solution concentration. This shows that the discrepancy between chromogenic and plasma-coagulation assays for *αFXIIa* in buffer solution is not due to autoamplification but rather an autohydrolysis reaction of the type suggested by the chemical formula *FXIIa* + *FXII* → amidolytic enzyme(s). High-resolution electrophoresis of autohydrolysis products did not show evidence of proteolytic cleavage of either

FXII or *αFXIIa*. We are thus led to hypothesize that the autohydrolysis reaction generates a change in conformation in either the *FXII* or *αFXIIa* molecule, which alters further *αFXIIa* procoagulant activity.

4.6 References

1. Vogler EA, Siedlecki CA. Contact Activation of Blood Plasma Coagulation: A Contribution from the Hematology at Biomaterial Interfaces Research Group the Pennsylvania State University. Biomaterials. 2009;30(10):1857-69.
2. Golas A, Parhi P, Dimachkie ZO, Siedlecki CA, Vogler EA. Surface-Energy Dependent Contact Activation of Blood Factor XII. Biomaterials. 2010;31(6):1068-79.
3. Golas A, Yeh CHJ, Siedlecki CA, Vogler EA. Amidolytic, Procoagulant, and Activation-Suppressing Proteins Produced by Contact Activation of Blood Factor XII in Buffer Solution. Biomaterials.32(36):9747-57.
4. Josh Yeh CH, Dimachkie ZO, Golas A, Cheng A, Parhi P, Vogler EA. Contact Activation of Blood Plasma and Factor XII by Ion-Exchange Resins. Biomaterials. 2012;33(1):9-19.
5. Golas A, Yeh CHJ, Pitakjakpipop H, Siedlecki CA, Vogler EA. A Comparison of Blood Factor XII Autoactivation in Buffer, Protein Cocktail, Serum, and Plasma Solutions. Biomaterials.34(3):607-20.
6. Fastrez J. Engineering Allosteric Regulation into Biological Catalysts. Chembiochem. 2009;10(18):2824-35.
7. McMillin CR, Saito H, Ratnoff OD, Walton AG. Secondary Structure of Human Hageman-Factor (Factor-XII) and Its Alteration by Activating Agents. Journal of Clinical Investigation. 1974;54(6):1312-22.
8. Revak SD, Cochrane CG, Bouma BN, Griffin JH. Surface and Fluid Phase Activities of 2 Forms of Activated Hageman-Factor Produced During Contact Activation of Plasma. Journal of Experimental Medicine. 1978;147(3):719-29.
9. Dunn JT, Silverberg M, Kaplan AP. The Cleavage and Formation of Activated Human Hageman Factor by Autodigestion and by Kallikrein. J Biol Chem. 1982;257(4):1779-84.
10. Silverberg M, Dunn JT, Garen L, Kaplan AP. Autoactivation of Human Hageman Factor. Demonstration Utilizing a Synthetic Substrate. J Biol Chem. 1980;255(15):7281-6.
11. Dunn JT, Silverberg M, Kaplan AP. Structural-Changes Accompanying Hageman-Factor Activation by Proteolysis. Clinical Research. 1982;30(2):A315-A.
12. Miller G, Silverberg M, Kaplan AP. Autoactivatability of Human Hageman-Factor (Factor-XII). Biochemical and Biophysical Research Communications. 1980;92(3):803-10.
13. Silverberg M, Kettner C, Shaw E, Kaplan AP. Enzymatic-Activities of Native and Activated Hageman-Factor (Hf). Circulation. 1980;62(4):57-.
14. Vanderkamp K, Vanoeveren W. Factor-XII Fragment and Kallikrein Generation in Plasma During Incubation with Biomaterials. Journal of Biomedical Materials Research. 1994;28(3):349-52.

15. Maas C, Oschatz C, Renne T. The Plasma Contact System 2.0. Seminars in Thrombosis and Hemostasis.37(4):375-81.
16. Samuel M, Pixley RA, Villanueva MA, Colman RW, Villanueva GB. Human Factor-XII (Hageman-Factor) Autoactivation by Dextran Sulfate - Circular-Dichroism, Fluorescence, and Ultraviolet Difference Spectroscopic Studies. Journal of Biological Chemistry. 1992;267(27):19691-7.
17. McMillin CR, Walton AG. Circular-Dichroism Technique for Study of Adsorbed Protein Structure. Journal of Colloid and Interface Science. 1974;48(2):345-9.
18. Griep M, Fujikawa K, Nelsestuen G. Possible Basis for the Apparent Surface Selectivity of the Contact Activation of Human-Blood Coagulation Factor-XII. Biochemistry. 1986;25(21):6688-94.
19. Samuel M, Samuel E, Villanueva GB. The Low Ph Stability of Human Coagulation-Factor-XII (Hageman-Factor) Is Due to Reversible Conformational Transitions. Thrombosis Research. 1994;75(3):259-68.
20. Ratnoff OD, Saito H. Amidolytic Properties of Single-Chain Activated Hageman-Factor. Proceedings of the National Academy of Sciences of the United States of America. 1979;76(3):1461-3.
21. Revak SD, Cochrane CG, Johnston AR, Hugli TE. Structural-Changes Accompanying Enzymatic Activation of Human Hageman-Factor. Journal of Clinical Investigation. 1974;54(3):619-27.
22. Pixley RA, Colman RW. Factor-XII - Hageman-Factor. Proteolytic Enzymes in Coagulation, Fibrinolysis, and Complement Activation, Part A. 1993;222:51-65.
23. Henriques ES, Floriano WB, Reuter N, Melo A, Brown D, Gomes J, et al. The Search for a New Model Structure of Beta-Factor Xiia. Journal of Computer-Aided Molecular Design. 2001;15(4):309-22.
24. Chatterjee K, Thornton JL, Bauer JW, Vogler EA, Siedlecki CA. Moderation of Prekallkrein-Factor XII Interactions in Surface Activation of Coagulation by Protein-Adsorption Competition. Biomaterials. 2009;30(28):4915-20.
25. Chatterjee K, Vogler EA, Siedlecki CA. Procoagulant Activity of Surface-Immobilized Hageman Factor. Biomaterials. 2006;27(33):5643-50.
26. Guo Z, Bussard KM, Chatterjee K, Miller R, Vogler EA, Siedlecki CA. Mathematical Modeling of Material-Induced Blood Plasma Coagulation. Biomaterials. 2006;27(5):796-806.
27. Friberger P. Synthetic Peptide Substrate Assays in Coagulation and Fibrinolysis and Their Application on Automates. Seminars in Thrombosis and Hemostasis. 1983;9(4):281-300.
28. Krishnan A, Liu YH, Cha P, Woodward R, Allara D, Vogler EA. An Evaluation of Methods for Contact Angle Measurement. Colloids and surfaces B, Biointerfaces. 2005;43(2):95-8.
29. Lander LM, Siewierski LM, Brittain WJ, Vogler EA. A Systematic Comparison of Contact Angle Methods. Langmuir. 1993;9(8):2237-9.
30. Parhi P, Golas A, Barnthip N, Noh H, Vogler EA. Volumetric Interpretation of Protein Adsorption: Capacity Scaling with Adsorbate Molecular Weight and Adsorbent Surface Energy. Biomaterials. 2009;30(36):6814-24.
31. MSW N. Application of the Experion Automated Electrophoresis System to Glycoprotein Visualization and Analysis: Bio_Rad Laboratories. 2007.
32. Espana F, Ratnoff OD. Activation of Hageman-Factor (Factor-XII) by Sulfatides and Other Agents in the Absence of Plasma Proteases. Journal of Laboratory and Clinical Medicine. 1983;102(1):31-45.
33. Revak SD, Cochrane CG, Griffin JH. The Binding and Cleavage Characteristics of Human Hageman Factor During Contact Activation: A Comparison of Normal Plasma with Plasmas

Deficient in Factor XI, Prekallikrein, or High Molecular Weight Kininogen. The Journal of Clinical Investigation. 1977;59(6):1167-75.
34. Dunn J, Kaplan A. Formation and Structure of Human Hageman-Factor Fragments. The Journal of clinical investigation. 1982;70(3):627-31.
35. Ratnoff OD. Studies on the Inhibition of Ellagic Acid Activated Hageman-Factor (Factor-XII) and Hageman-Factor Fragments. Blood. 1981;57(1):55-8.
36. Ratnoff OD. The Relative Amidolytic Activity of Hageman-Factor (Factor-XII) and Its Fragments - the Effect of High-Molecular-Weight Kininogen and Kaolin. Journal of Laboratory and Clinical Medicine. 1980;96(2):267-77.
37. Wuepper KD, Cochrane CG. Effect of Plasma Kallikrein on Coagulation *in-vitro*. Proceedings of the Society for Experimental Biology and Medicine. 1972;141(1):271-&.
38. Chatterjee K, Guo Z, Vogle EA, Siedlecki CA. Contributions of Contact Activation Pathways of Coagulation Factor XII in Plasma. Journal of Biomedical Materials Research Part A. 2009;90A(1):27-34.
39. Zhuo R, Vogler EA. Practical Application of a Chromogenic FXIIa Assay. Biomaterials. 2006;27(28):4840-5.
40. Colman R, Wachtfogel Y, Kucich U, Weinbaum G, Hahn S, Pixley R, et al. Effect of Cleavage of the Heavy Chain of Human Plasma Kallikrein on Its Functional Properties. Blood. 1985;65(2):311-8.
41. Revak SD, Cochrane CG, Griffin JH. Multiple Forms of Active Hageman-Factor (Hf) (Coagulation Factor-XII) Produced During Contact Activation. Federation Proceedings. 1977;36(3):329-.
42. Revak SD, Cochrane CG. Hageman-Factor - Its Structure and Modes of Activation. Thrombosis and Haemostasis. 1976;35(3):570-5.
43. Revak SD, Cochrane CG, Griffin JH. Plasma-Proteins Necessary for Cleavage of Human Hageman-Factor During Surface Activation. Federation Proceedings. 1976;35(3):692-.
44. Ratnoff OD, Saito H. The Evolution of Clot-Promoting and Amidolytic Activities in Mixtures of Hageman-Factor (Factor-XII) and Ellagic Acid - the Enhancing Effect of Other Proteins. Journal of Laboratory and Clinical Medicine. 1982;100(2):248-60.
45. Heimark RL, Kurachi K, Fujikawa K, Davie EW. Surface Activation of Blood-Coagulation, Fibrinolysis and Kinin Formation. Nature. 1980;286(5772):456-60.
46. Citarella F, Wuillemin WA, Lubbers YTP, Hack CE. Initiation of Contact System Activation in Plasma Is Dependent on Factor XII Autoactivation and Not on Enhanced Susceptibility of Factor XII for Kallikrein Cleavage. British Journal of Haematology. 1997;99(1):197-205.
47. Zhuo R, Siedlecki CA, Vogler EA. Autoactivation of Blood Factor XII at Hydrophilic and Hydrophobic Surfaces. Biomaterials. 2006;27(24):4325-32.
48. Vogler EA. Protein Adsorption in Three Dimensions. Biomaterials. 2012;33(5):1201-37.

Chapter 5

Conclusion

5.1 Summary and Conclusions

Potential development of sophisticated cardiovascular biomaterials requires structure-property relationship linking blood coagulation with material properties such as surface chemistry/energy. However, three key discoveries have been made in this work that significantly improve our core understanding of contact activation and revises the extant paradigm of plasma coagulation.

1. We propose that this thrombin amplification route is catalyzed by the substantial amount of *FIIa* generated in coagulating plasma that persists in serum prepared from coagulated plasma. However, it does not afford proper emphasis as a pivotal feedback loop that activates *FXI in vitro*, in a way similar to that known to occur *in vivo*. Thus, a connection between *in vitro* and *in vivo* coagulation is drawn.
2. The following investigation includes an updated version of the contact activation phase mediated by surface activation of Hageman factor *FXII* and emphasizes a role for *FXI* in controlling the time required to complete plasma coagulation after activation with hydrophilic procoagulant surfaces.
3. The autoactivation creates an ensemble of single-chain active *FXII* conformers. These conformers may possibly be an intermediate step in the contact-activation reactions as they

undergo proteolytic cleavage in the presence of prekallikrein and high-molecular weight kininogen, as suggested by earlier investigators.

4. The procoagulant activity measured by a plasma-coagulation assay decreases systematically with increasing *FXII* solution concentration. This implies that *αFXIIa* activity is inhibited by an unknown reaction between *FXII* and *αFXIIa*. Under the same reaction conditions, chromogenic assay (s-2303 chromogen) reveals that net amidolytic activity increases with increasing *FXII* solution concentration. From unrelated result, we are thus led to hypothesize that the autohydrolysis reaction generates a change in conformation in either the *FXII* or *αFXIIa* molecule, which alters further *αFXIIa* procoagulant activity in buffer.

5.2 Future Work

The following areas of future work have been identified during this thesis.

First, high resolution electrophoresis will have to be investigated in order to quantify the mass distribution of fragments produced by autoactivation of *FXII* in the presence of prekallikrein and high-molecular weight kininogen, *FXIIa, FXI* and thrombin(*FIIa*).

Secondly, blood-plasma coagulation assays will be tested on biomaterial devices to examine hemocompatibility and ultimately lead to proper design surface chemistry/energy for the particular patient.

Finally, a mathematical model of blood coagulation will be developed from the revised version of the blood coagulation cascade. Therefore, if we know a patient’s blood factor concentrations, we can design a medical device appropriate for patient's age and activities.

Appendix A

3D Crystal Structures of Blood Coagulation Factors

The 3D crystal structures of blood coagulation factors are generated from RCSB Protein Data Bank website (http://www.rcsb.org) by using the Macromolecular Transmission Format (MMTF) for 3D visualization and analysis.

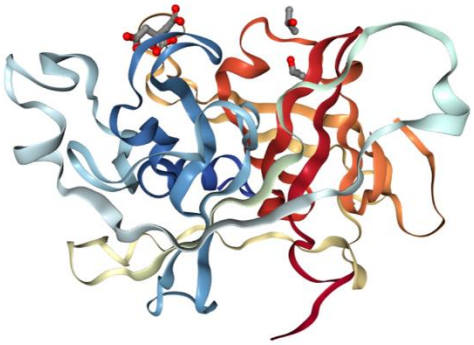

Figure A-1. Factor XII

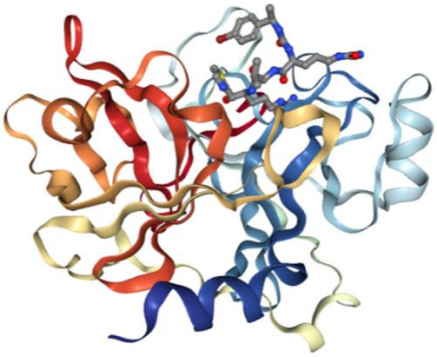

Figure A-2. Factor XI

Figure A-3. Factor X

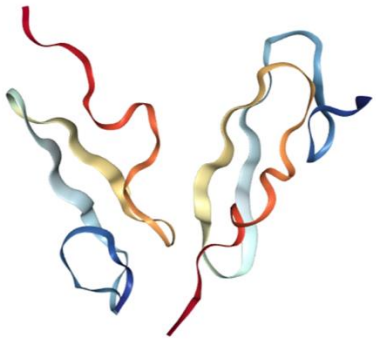

Figure A-4. Factor IX

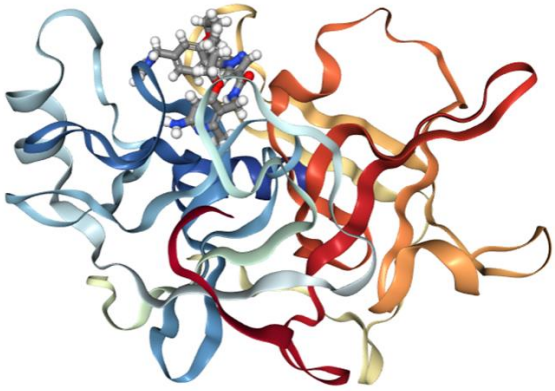

Figure A-5. Prekallikrein

Appendix B

Autoactivation Yield in Plasma Estimated from FXIIa Titration

FXIIa titrations of plasma used in this work were change from normal plot of [FXII] to linear-like on a log[$FXIIa$] scale over the coagulation time (CT) range of interest (see Fig.4.6), where $[FXIIa]_{ex}$ the exogenous *FXIIa* titrant concentration expressed in PEU/mL is prepared by serial dilutions of purified *FXIIa* solutions of known concentration. Linear regression through the linear-like range yields:

$$y = m\log_{10}[FXIIa]_{ex} + b \qquad \text{Eq. 1}$$

The linear regression parameters m and c (Microsoft Excel) correspond to the slope and intercept of the linear-like range of the exogenous FXIIa titration curve, respectively. Equation 1 is an approximation that implicitly assumes the contribution of reciprocal-loop amplification of the exogenous bolus is small relative to $[FXIIa]_{ex}$. An explicit accounting of reciprocal-loop amplification requires Eq. (1) to be re-written as:

$$y = m\log_{10}[FXIIa]_{tot} + b \qquad \text{Eq.2}$$

where $[FXIIa]_{tot} = [FXIIa]_{ex} + \alpha_{RL}[FXIIa]_{ex}$ and α_{RL} is the reciprocal-loop amplification factor. The slope and intercept are the same as in Eq. (1) because the observed CT actually depends on the sum of exogenous and endogenous *FXIIa* contributions. Based on the work of Chatterjee et al, α_{RL} is assumed to be a constant factor over the linear-like range of a *FXIIa* titration. Eq. (2) can be used to determine an unknown amount of *FXIIa* in a test solution added to plasma if two additional assumptions are made. The first assumption is that an unknown *FXIIa* concentration $[FXIIa]_{uk}$ in a test solution is amplified by the same reciprocal-loop amplification factor α_{RL}as in *FXIIa* titration of plasma. Such test solutions might be obtained by autoactivation of exogenous

FXII in PBS solution or autoactivation of endogenous *FXII* in plasma by surface-area titration (SAT). Again, taking reciprocal-loop amplification explicitly into account, $[FXIIa]_{uk\,tot} = ([FXIIa]_{ex} + \alpha_{RL}[FXIIa]_{uk})$ where $[FXIIa]_{uk\,tot}$ is the total unknown concentration of *FXIIa* causing plasma to coagulate at a particular measured CT.

The second assumption is that a particular plasma CT occurs at a unique total FXIIa concentration independent of how that *FXIIa* was generated in plasma. In other words, a particular CT caused by activation of endogenous *FXII* in a plasma SAT is due to exactly the same total *FXIIa* concentration as that causing the same CT in an *FXIIa* titration or by addition of a solution containing an unknown *FXIIa* concentration to plasma. With these underlying assumptions in mind, the mass balance of Eq. (3) holds for a specific CT caused by an unknown *FXIIa* concentration and exogenous *FXIIa* titration:

$$[FXIIa]_{uk\,tot} = ([FXIIa]_{uk} + \alpha_{RL}[FXIIa]_{uk}) = [FXIIa]_{tot} = ([FXIIa]_{ex} + \alpha_{RL}[FXIIa]_{ex})$$

$$[FXIIa]_{uk} = [FXIIa]_{ex} \qquad \text{Eq.3}$$

Thus, unknown *FXIIa* concentrations in plasma can be determined by equating equivalent CT obtained by *FXIIa* titration of that plasma. An example calculation for the unknown *FXIIa* concentration for autoactivation as well as uncertainty is provided in Appendix C

Appendix C

Calculation of unknown activation factor with propagation of error

Propagation of error is the effect of variables' uncertainty (or error), on the uncertainty of a function based on them. *FXIIa* yields were calculated from calibration curves that were fit to

$y = m\log_{10} x + b$ $(where\ y = coagulation\ time, x = [FXIIa])$ by linear least squares regression. Uncertainty in calculated[FXIIa] was determined using the following general formula for propagation of error using partial derivatives:

$$\sigma_y = \sqrt{\left(\frac{\partial y}{\partial a}\right)^2 (\sigma_a)^2 + \left(\frac{\partial y}{\partial b}\right)^2 (\sigma_b)^2 + \left(\frac{\partial y}{\partial c}\right)^2 (\sigma_c)^2}$$

From Eq.1, Appendix B, uncertainty in [FXIIa] (to account for uncertainty of fit) was thus determined as:

$$\sigma_{[FXIIa]} = \sqrt{\left(\frac{\partial [FXII]}{\partial m}\right)^2 (\sigma_m)^2 + \left(\frac{\partial y}{\partial c}\right)^2 (\sigma_b)^2}$$

The blood plasma coagulation assay to measure the clot time of each concentration of *FXIIa* gives;

Concentration *FXIIa* of (PEU/ml)	Clot time (min.)	Log[FXIIa]
2	6.90	0.301
1	7.67	0
0.5	11.47	-0.301
0.25	14.85	-0.602
0.125	19.85	-0.903
0.0625	22.67	-1.204
0.0313	24.92	-1.505
0.0156	26.12	-1.806
0.0078	27.72	-2.107
0.0039	29.25	-2.408
0.00195	33.37	-2.709

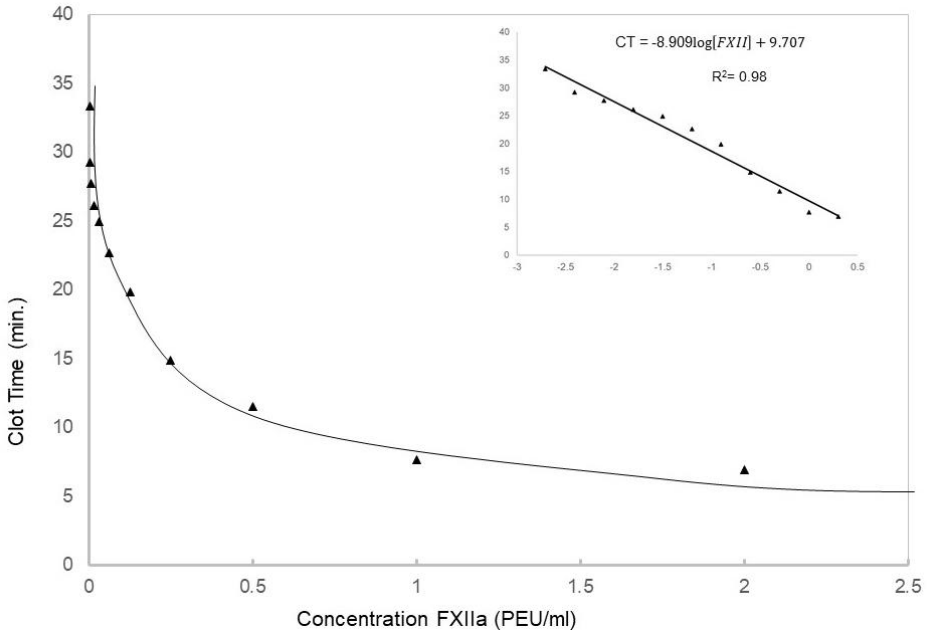

Figure A *FXIIa* titration of human plasma, plotting observed plasma coagulation time (CT, ordinate) against exogenous *FXIIa* concentration (abscissa). The asymptotic curve is linear on logarithmic axes (inset), creating a convenient calibration curve that allows estimation of apparent *FXIIa* concentration from measured Clot Time. Lines through the data are guides to the eye.
Using Regression Statistics of Microsoft Excel to get m, σ_m, b and σ_b ($m = -8.909, \sigma_m$ 0.498, $b = 9.707, \sigma_b = 0.765$).

Regression Statistics								
Multiple R	0.990460101							
R Square	0.981011212							
Adjusted R Square	0.977846414							
Standard Error	0.786220125							
Observations	8							
ANOVA								
	df	*SS*	*MS*	*F*	*Significance F*			
Regression	1	191.6091683	191.6091683	309.9759308	2.15506E-06			
Residual	6	3.708852513	0.618142086					
Total	7	195.3180208						
	Coefficients	*Standard Error*	*t Stat*	*P-value*	*Lower 95%*	*Upper 95%*	*Lower 95.0%*	*Upper 95.0%*
Intercept	7.345634921	0.411403926	17.85504333	1.9837E-06	6.338965779	8.352304062	6.338965779	8.352304062
X Variable 1	-7.095348401	0.403004355	-17.60613333	2.15506E-06	-8.081464533	-6.109232269	-8.081464533	-6.109232269

m = -7.095, σ_m= 0.403, b = 7.346, σ_b= 0.411

Appendix D Schematic of Silane molecular structures

1. OTS(octadecyltricholorosilane)

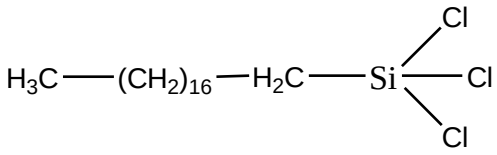

2. Nyebar (1,1-pentadecafluro octylmethacrylate)

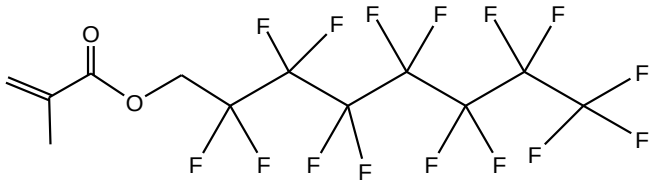

3. APTES(aminopropyltriethoxysilane)